AD-A147 196 EVALUATION OF JET FUEL DEPOSIT KINETICS LOT IV(U) PRATT 1/1
AND WHITNEY WEST PALM BEACH FL GOVERNMENT PRODUCTS DIV
W J PURVIS ET AL. MAR 84 PWA-FR-17658 NAPC-PE-107C
UNCLASSIFIED N00140-80-C-0097 F/G 21/4 NL

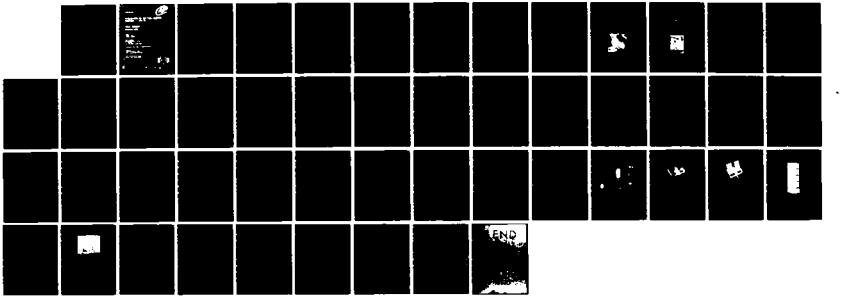

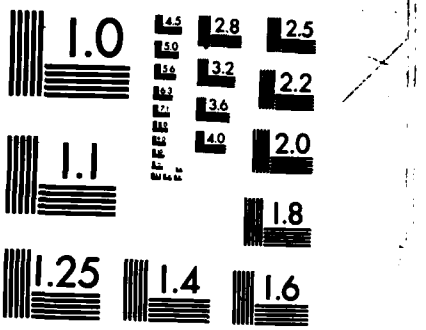
1.0
1.1
1.25
1.4
1.6
1.8
2.0
2.2
2.5
2.8
3.2
3.6
4.0
4.5
5.0

UNCLASSIFIED

SECURITY CLASSIFICATION OF THIS PAGE (When Data Entered)

REPORT DOCUMENTATION PAGE

READ INSTRUCTIONS BEFORE COMPLETING FORM

1. REPORT NUMBER: NAPC-PE-107C	2. GOVT ACCESSION NO.
3. RECIPIENT'S CATALOG NUMBER	
4. TITLE (and Subtitle): Evaluation of Jet Fuel Deposit Kinetics - Lot IV	5. TYPE OF REPORT & PERIOD COVERED: Final Report, March 1983 - March 1984
6. PERFORMING ORG. REPORT NUMBER: FR-17658	
7. AUTHOR(s): William J. Purvis, Richard J. Meehan	8. CONTRACT OR GRANT NUMBER(s): N00140-80-C-0097
9. PERFORMING ORGANIZATION NAME AND ADDRESS: Pratt & Whitney, Government Products Division, P. O. Box 2691, West Palm Beach, Florida 33402	10. PROGRAM ELEMENT, PROJECT, TASK AREA & WORK UNIT NUMBERS
11. CONTROLLING OFFICE NAME AND ADDRESS: Naval Air Propulsion Center, Trenton, New Jersey 08628	12. REPORT DATE: March 1984
	13. NUMBER OF PAGES: 41
14. MONITORING AGENCY NAME & ADDRESS(if different from Controlling Office)	15. SECURITY CLASS. (of this report): Unclassified
	15a. DECLASSIFICATION/DOWNGRADING SCHEDULE

16. DISTRIBUTION STATEMENT (of this Report)
Approved for Public Release, Distribution Unlimited

17. DISTRIBUTION STATEMENT (of the abstract entered in Block 20, if different from Report)

18. SUPPLEMENTARY NOTES

19. KEY WORDS (Continue on reverse side if necessary and identify by block number)
Coking
JP-5 Fuel
Deposition
JFTOT

20. ABSTRACT (Continue on reverse side if necessary and identify by block number)
An investigation of a visual method for the continuous measurement of jet fuel deposition was conducted using a modified JFTOT. A modified ASTM D-3241 procedure was developed and a remote reflectant probe was used to establish variations and fuel depositions for four Navy jet fuels. Arrhenius plots and activation energies were calculated based on the time-to-TDR versus temperature data.

DD FORM 1 JAN 73 1473 EDITION OF 1 NOV 65 IS OBSOLETE
S/N 0102-014-6601 |

UNCLASSIFIED

SECURITY CLASSIFICATION OF THIS PAGE (When Data Entered)

Contents

Illustrations

Illustrations (Continued)

Tables

ABSTRACT

Four selected JP-5 type fuels were investigated with regard to their rate of thermally induced deposition using two analytical techniques. A modified research Jet Fuel Thermal Oxidation Tester (JFTOT), using a quartz-enclosed heater section in combination with a photosensitive detector, was used to monitor the buildup of thermally induced fuel deposits. Concurrent with the JFTOT, tests were conducted using the Experimental Coking Apparatus (ECA) in order to establish comparable deposition rate data. The resultant Arrhenius analyses have contributed to understanding the impact of an invariant oxygen concentration on the specific fuel deposition rate. An attempt to measure the hydrocarbon peroxide associated with each fuel and the buildup of organo-peroxide with fuel temperature was inconclusive due to the variation in peroxide potential analysis (ASTM D-3703).

Navy jet

Orig. for-supplied Key words include: Coking.

SECTION I
INTRODUCTION

Petroleum-derived jet fuels have, since their basic inception, demonstrated widespread and varying degrees of thermal stability. Current jet fuel laboratories use the Jet Fuel Thermal Oxidation Tester (JFTOT) (ASTM D-3241) to rate fuels primarily with a go, no go criteria which, as such, is relatively limited in relation to actual thermal stability considerations.

Thermal instability can be regarded as the inability of a jet fuel to withstand thermally induced oxidation that may result in molecular rearrangement with the potential formation of fuel deposits. This instability may result in polymerization of fuel materials and a subsequent formation of a varnish type deposit. Thermal instability adversely affects fuel system controls, filters, operational valves and manifolds with an ultimate impact on aircraft maintainability, operational functionality and overall unit cost.

The purpose of this fuel study was to establish the operational feasibility of a modified JFTOT for evaluating fuel deposit formation as a function of temperature. The JFTOT and the Experimental Coking Apparatus (ECA)[1], developed at Pratt & Whitney, Florida, were used to generate the data for temperature-dependent Arrhenius plots and subsequent calculations of the activation energy for the thermal deposition of each fuel. In addition to deposition data, each of the four Navy supplied fuels was thermally stressed and evaluated to determine its peroxide formation potential. From these data, an attempt was made to evaluate each fuel's activation energy. The following section describes the three tasks of this study: (1) the modified JFTOT method, (2) the ECA, and (3) fuel peroxide level after thermal stressing. During these fuel stability experiments, an attempt was made to obtain consistent deposition rate data and, from these data, to derive an overall Arrhenius evaluation under conditions of steady oxygen supply.

The research JFTOT, with its associated peripheral equipment, was significantly modified from the ASTM D-3241 in order to allow continuous monitoring of each fuel's deposition on standard heater tubes. The heart of the modification was the use of the remote, light-emitting, photosensitive probe. By measuring changes in light reflected from the surface of the heater tube, this modification allowed the deposit to be evaluated as the test conditions and fuel oxidation progressed measurement of the time dependency for attaining a specific tube rating allowed an Arrhenius plot to be produced for each fuel. From this plot, the slope and intercept for the Arrhenius evaluation was established. The ECA also provided a similar type of analysis by the gravimetric evaluation of steel coupons used to collect the polymerized fuel deposits formed at specific fuel test temperatures. The ECA provided data that reflects the effect of a pseudo first-order reaction, first order in fuel concentration because the oxygen concentration during the test was held constant at 21 percent. Prior to this study, both of these methods had been used in preliminary investigations to determine the Arrhenius activation energies of jet fuels. In addition to these two methods, the determination of each fuel's peroxide concentration level, both before and after a thermal stress, was made. These data, derived over the same temperature range established in the ECA tests, were used in an attempt to develop Arrhenius plots. This approach may ultimately provide another method of establishing a fuel's activation energy, one that is directly related to the proposed chemical mechanism of the deposit formation.

[1] Refer to Appendix A for a detailed discussion of the ECA.

SECTION II
TECHNICAL DISCUSSION

A. JET FUEL THERMAL OXIDATION TESTER (MODIFIED)

This program used a modified Jet Fuel Thermal Oxidation Tester (JFTOT) heater section to study deposit formation as a function of time at various temperature levels. The modification of the heater test section consisted of using a three-inch section of quartz tubing as the outer wall in place of the standard stainless steel wall. A remote light reflectance probe, SKAN-102, was attached to the modified section and focused on the empirically established hot spot of the aluminum heater tube. Figure II-1 shows the remote probe and its transparent heater tube section. The remote probe, by means of a four-wire umbilical cord, was electrically connected to a modified Mark VIII A Tuberator. As high-temperature testing progressed, a deposit buildup was monitored on the aluminum heater tube by the remote probe and was observed by the meter deflection of the Mark VIII A Tuberator. Figure II-2 shows a heat tube after a six-hour test at 288°C with JP-5 fuel. This meter deflection provided an electrical impulse signal to a strip chart recorder. The recorder was set on a sensitivity of 10 millivolts full scale and a chart speed of 4 inches per hour. The trace recording derived from these recorder parameters produces a graphic picture of deposit buildup as a function of time and temperature.

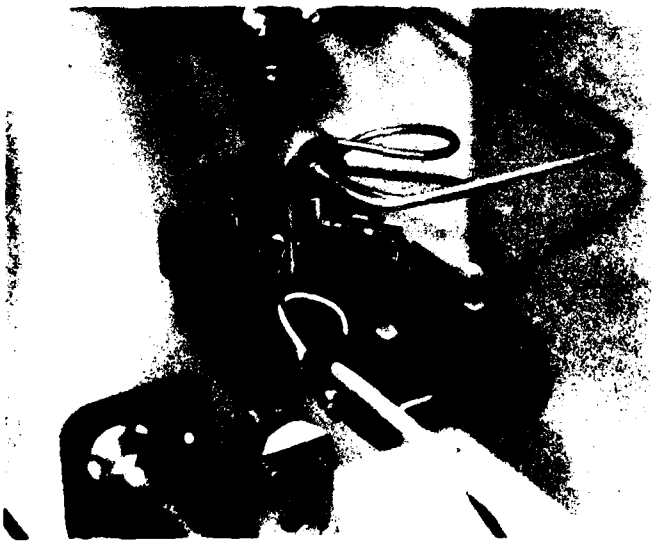

FE 355259-6

Figure II-1. Remote Probe and Transparent Heater Tube Section

The JFTOT used for this program is a specially built apparatus manufactured by Inter Av™ and has capabilities beyond those of the standard JFTOT. Figure II-3 shows the JFTOT with the remote probe and TDR. Tests runs of 1000 minutes' duration can be made at the standard flow rate of 3.0 milliliters (mL) per minute. The flow rate can be set to run at any interval from 1.0 to 10 mL per minute at pressures to 1000 pounds per square inch gauge (psig) and 427°C (800°F).

FE 355081-3

Figure II-2. Heat Tube After Six-Hour Test at 288°C With JP-5 Fuel

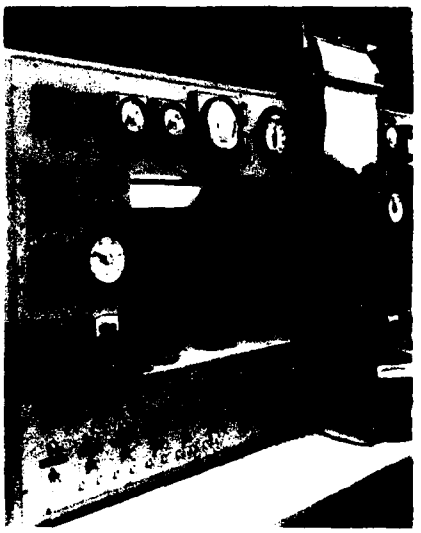

FC 46174

Figure II-3. JFTOT With Remote Probe and TDR

B. QUARTZ-ENCLOSED TEST SECTION JFTOT ANALYSIS

This study entailed the use of two different sizes of bulk fuel reservoirs. When JFTOT runs were made at higher temperatures, the standard 1#L reservoir was used since the runs were terminated before 1000 mL of fuel had been consumed. Lower temperature runs, where the use of more than 1000 mL of fuel was predicted, employed a 3#L fuel reservoir. If a 3000-mL charge of fuel was to be used, a deviation in the ASTM D-3241 procedure for fuel aeration was used. The

normal aeration time of 6 minutes for a 1000-mL fuel charge was extended to 15 minutes for a 3000-mL fuel charge.

The first several runs were made using pyrex glass as the outer wall of the test section. When high precision quartz tubing became available, all subsequent runs employed the quartz tubing. Early in the program, some runs were aborted due to unexplained fluctuations of the indicating needle of the Mark VIII A Tuberator. The reason for these fluctuations has not been discovered. These fluctuations were, however, only a temporary anomaly and did not influence the test data.

During the early stage of the program, the negative deflection of the TDR indicating needle, which occurred when the tube heater was energized, caused considerable concern. Remedial action was taken by using the Lo Cal meter adjustment knob to return the needle to the ZERO position. A decision was made to disregard the negative deflection and continue the run without adjusting the meter. All test runs included in this report were made without resetting the meter to the ZERO position.

As test run time proceeded, the indicating needle slowly returned to ZERO; as deposit formation started, the meter reading climbed as light reflectance diminished. During the test cycle, observations of meter reading were observed and recorded at 15-minute intervals. Since these observations required almost constant observation of the apparatus, a decision was made to incorporate a strip chart recorder into the system.

Appropriate signal pickup receptacles were installed in the Mark VIII A Tuberator, and the Tuberator was connected to a Hewlett Packard Model 7132A strip chart recorder. During preliminary testing of the recording Tuberator, the recorder was set at a sensitivity of 50 mV and a chart speed of 6 inches per hour. These recorder settings did not produce a satisfactory trace because the high mV setting was not sensitive enough to provide a well defined spacing between increments of one number on the TDR meter. Also, the length of the recorder trace on the chart paper was prohibitive. Accordingly, the sensitivity of the recorder was increased by using a setting of 10 mV full scale, and the chart speed decreased to 4 inches per hour. Linearity between the Mark VIII A Tuberator and the recorder was established as described in Appendix C, Section 3.

Incorporation of the strip chart recorder into the deposit measuring apparatus proved to be an invaluable tool. The continuous trace of the recorder eliminated the requirement of having personnel in constant attendance and provided a post test reference to any anomalies during the test. It was observed that, during about 95% of the runs, a definite decrease in deposit formation growth appeared to occur as the indicating meter approached a TDR number of 8 to 10. During this time, the recorder trace started to flatten out and then decreased slowly, over a period of 30 to 45 minutes, from 1 to 1½ TDR numbers. At the end of this period, the meter reading started slowly rising again and a subsequent change showed on the recorder trace.

This apparent decrease in the deposit formation rate has been difficult to explain. The consensus of opinion is that the light-reflectance probe inherently fails to distinguish between shiny and dull deposit finishes. It is theorized that the initial deposit formation formed on the shiny heater tube presents a dull finish to the reflectance probe. As test time progresses, the continued heat input from the heater tube hardens this deposit, thereby changing the tubes surface appearance from dull to shiny. Prior experience indicates that a dull surface finish produces a higher TDR number and a shiny surface finish produces a lower TDR number.

One primary cause of concern during this program was the validity of data regarding the magnitude of deposit buildup as a function of time versus temperature. The SPOT TDR number of 15 was arbitrarily selected as an indication of failure for this program. The length of all runs

was predicated on the time required at temperature for the TDR probe to exhibit a meter reading of 15. The remote probe was positioned 38.7 mm downstream of the point of fuel entry to the heated test section. When the heater tube was examined following a test run, darker deposits were often noted downstream of the remote probe location. Also, darker areas were sometimes noted at the 38.7 mm plane of the tube, but 180 degrees removed from the probe focal point. Logically, a higher magnitude of deposit formation would be expected to occur at the hottest spot (assuming constant wall thickness) on the tube (i.e., the 38.7 mm zone monitored). The scatter in the exact position of the higher deposits raises the possibility that a minute difference in surface finish of the tube could cause these anomalies. A more extensive investigation will be required to furnish a complete explanation of these observations.

Table II-1 lists the physical properties of the four fuels as measured at the onset of this study and the most recent Navy data. Most of the physical properties are consistent, except for the volume percent (v/o) of aromatic materials found in NAPC-5. The Fuel Laboratory at the Pratt and Whitney Government Products Division (P&W/GPD) evaluated the aromatic concentration as 22 v/o compared to 15 v/o found in the Navy analysis. This inconsistency was found to be caused by a fuel shipment error. In cases where the distillation residue was greater in one analysis than in another, the lower value is due to the higher end point temperature. The higher residual from distillation was probably due to use of a decomposition end point, rather than the end point or final boiling point, as the distillation end point.

Fuel studies that directly involve the thermal stability of aviation fuels may reflect erroneous data if the fuels' breakpoint temperature varies during a prolonged or extended study. In order to prevent this misinterpretation, a breakpoint temperature for each fuel used in this investigation was determined prior to the start of the fuel tests and after the final test. The before and after program breakpoint temperatures for each fuel are listed in Tables II-2 and II-3, respectively. All fuels were shown to be consistent through the testing period except NAPC-5. The NAPC-5 breakpoint temperature reflects a decrease in the fuel's thermal stability. This decrease would explain any subsequent difficulty in establishing acceptable modified JFTOT test results. It was concluded, based on the observed change in breakpoint temperature, that the quality of the NAPC-5 fuel changed during the duration of this study.

The JFTOT fuel temperatures, as run by the standard procedure ASTM D-3241-82 (IP 323/75), are listed in Table II-2. The breakpoint temperature was established to within 6°C. These data are presented in the form of: (1) differential pressure drop (e.g. time in minutes to reach the recorded pressure drop), and (2) visual heater tube code rating (e.g. TDR spot rating).

In the modified JFTOT runs, the NAPC-5 fuel was initially run using the time to TDR 15 as the primary test index. It was not the intent to use TDR 15 as an absolute TDR, but to initiate these data and to review strip chart traces to determine a reliable and effective TDR value for all fuels in this study. For all NAPC-5 test temperatures, the variations of time to TDR, as related to TDR's of 3, 6, 9 and 12, are listed at the bottom of Table II-4.

Figure II-4 shows an actual TDR versus time data plot for the NAPC-5 fuel tests conducted at 282°C (540°F). These two tests were made early in the program during the final system checkout and before it was established that the thermal stability of the JP-5, NAPC-5 fuel had changed during storage. The exact breakpoint of the NAPC-5 during any given program test is not known; the initial breakpoint was 282°C (540°F). At the conclusion of this study, each fuel breakpoint temperature was re-established; the NAPC-5 breakpoint was found to be 260°C (500°F). This decrease in breakpoint with time indicates the storage stability of this fuel to be subject to change. Figure II-5 is a composite data plot showing a series of NAPC-5 tests at 282, 288, 293 and 299°C that were conducted after the determination of the fuel's thermal stability variation. These tests were conducted with a minimum of 24 hours between tests in order to establish comparable specific rates. Figures II-6, II-7 and II-8 are equivalent data plots for

NAPC-7, -11 and -14 at temperatures found to be within the range of each fuel's thermal breakpoint temperature. Variations of +11 and +22 degrees centigrade above the breakpoint and −5.5 and −11 degrees centigrade below the breakpoint were established in this study so that reasonable, but not excessive, time would be required for each modified JFTOT test.

Table II-1. Physical Properties of Fuel for Navy Program

	NAPC-JP-5		*NAPC-7*		*NAPC-11*		*NAPC-14*	
	GPD	*Navy*	*GPD*	*Navy*	*GPD*	*Navy*	*GPD*	*Navy*
API Gr/60F	40.8	41.8	35.7	35.6	39.7	39.6	43.7	43.7
Sp Gr/60F	0.8212	0.8165	0.8463	0.8468	0.8265	0.8270	0.8076	0.8076
Distillation, C (F)								
IBP	184 (364)	181 (358)	186 (366)	193 (379)	183 (361)	187 (369)	182 (359)	184 (363)
10%	198 (388)	199 (390)	200 (392)	204 (399)	203 (397)	205 (401)	191 (376)	193 (379)
20%	203 (397)	203 (397)	206 (403)	209 (408)	211 (412)	213 (415)	193 (380)	196 (385)
30%	206 (403)	—	211 (411)	—	218 (424)	—	196 (385)	—
40%	209 (408)	—	216 (421)	—	225 (437)	—	199 (390)	—
50%	213 (416)	217 (423)	221 (430)	226 (439)	233 (451)	233 (451)	202 (396)	205 (401)
60%	217 (422)	—	227 (441)	—	242 (468)	—	207 (404)	—
70%	222 (431)	—	235 (455)	—	253 (487)	—	211 (412)	—
80%	228 (442)	—	245 (473)	—	268 (514)	—	217 (423)	—
90%	238 (460)	243 (469)	266 (511)	272 (522)	294 (561)	294 (561)	227 (440)	231 (448)
End Point	262 (503)	261 (502)	326 (619)	288 (550)	333 (631)	304 (550)	247 (477)	257 (495)
Residue, %	1.1	1.2	1.7	3.6	1.5	6.0	0.8	1.2
Loss, %	0.9	0.2	0.8	0.4	0.5	—	0.7	0.4
Aromatics, v/o	22.2	14.99	33.6	32.57	21.1	21.6	22.6	24.0
Olefins, v/o	0.84	0.79	1.3	0.86	1.7	1.1	1.9	1.6
VIS/100F, cSt	1.57	1.58	1.81	1.77	2.03	1.98	1.41	1.38
Hydrogen, w/o	13.64	—	12.80	—	13.52	—	13.71	—
WSIM, MSS	81	85	33	22	<0	—	66	98
Critical Pressure (psi)	333		335		296		333	

Tables II-5 through II-8 list data generated by the quartz tube tests conducted on NAPC-5, 7, 11 and 14 fuels respectively. These data may be used to tabulate the time required for the system to reach a specific TDR. These data were compared at the conclusion of the last test, and a TDR of six was determined to be acceptable for the four fuels tested in this program.

Table II-2. Determination of Fuel Breakpoint Temperatures Standard JFTOT Runs on NAPC Fuels Showing Differential Pressure, Visual Code, Spot TDR|

Temperature, C (F)	*NAPC-7*	*NAPC-11*	*NAPC-14*		*NAPC-5*	
232.2 (450)		0/150 <2/2+				
237.8 (460)		0/150 2/7+				
243.3 (470)		0/150 <3/19.5		0/150* 1/7		
246.1 (475)	0/150 <3/17					
251.7 (485)	0/150 3/16			0/150* 2/6		
260 (500)	0/150 <4/18+		75/137 bypassed 1/3	0/150 <1/<0	0/150* 4/20*	0/150* 3/20*
271.1 (520)			8/150 1/4+	0/150* 4/23		
279.4 (535)			50/101 bypass 4/12	0/150* 4P/30		
282.2 (540)			80/106 bypass 4P/19	0/150 1/5	0/150 3P/10	0/150 <4/15
286.7 (548)				0/150 3P/28.5		
287.8 (550)			50/114 bypass 4P/21			
290.6 (555)				0/150 3P/26		

| Data Is in the Form of Differential Pressure/Minutes to ΔP; Visual Heater Code/TDR
* Data Established at the End of the Program

Table II-3. Fuel Breakpoint Determinations Standard JFTOT Run Used to Establish the Breakpoint Temperatures

Fuel	Test Parameters	*Pressure Drop* mm Hg/min	*Preheater Code* Visual	TDR-Spun	TDR-Spot
NAPC-7	Ambient/500F/150 min	0/150	<4	15	18
NAPC-7	Ambient/485F/150 min	0/150	3	15	16
NAPC-7	Ambient/475F/150 min	0/150	<3	15	17
NAPC-11	Ambient/470F/150 min	0/150	<3	17.5	19.5
NAPC-11	Ambient/460F/150 min	0/150	2	5	7
NAPC-11	Ambient/450F/150 min	0/150	<2	1	2
NAPC-14	Ambient/550F/150 min	25/105	4P	16	21
NAPC-14	Ambient/540F/150 min	80/106	>4P	15	19
NAPC-14	Ambient/535F/150 min	25/94	4	6	12
NAPC-14	Ambient/520F/150 min	8/150	1	1	4
NAPC-14	Ambient/500F/150 min	25/126	1	1	6
NAPC-5	Ambient/555F/150 min	0/150	3P	23	26
NAPC-5	Ambient/548F/150 min	0/150	3P	20	28.5
NAPC-5	Ambient/540F/150 min	0/150	1	1.5	5
NAPC-5	Ambient/500F/150 min	0/150	<1	<0	<0
NAPC-5	Ambient/540F/150 min	0/150	3P	5	10
NAPC-5	Ambient/540F/150 min	0/150	<4	15	26
NAPC-5	Ambient/535F/150 min	0/150	4P	24	30
NAPC-5	Ambient/525F/150 min	0/150	4P	14.5	23
NAPC-5	Ambient/520F/150 min	0/150	4P	16	22
NAPC-5	Ambient/500F/150 min	0/150	4P	21	22
NAPC-5	Ambient/470F/150 min	0/150	1	4.5	7
NAPC-5	Ambient/485F/150 min	0/150	2	5	6
NAPC-5	Ambient/500F/150 min	0/150	3	16.5	20

*Table II-4. NAPC-5 Fuel Time, Minutes Per TDR Reading to Attain a TDR Reading of 15.0**

Time Minutes	*530F*	*540F*	*No. 1 550F*	*No. 2 550F*	*560F*	*No. 1 570F*	*No. 2 570F*
0	0	0	0	0	0	0	0
5	0	−1.0	−0.5	−0.5	−0.5	0	−0.5
10	>0	<0	0.5	>0	0.5	<1	0.5
15	0.5	<1	2.0	>1	2.0	3	>2
20	>1	1.0	<4	3.0	<5	5.5	4.5
25	2.5	<3	>7	6.0	7	7.5	>7
30	4.0	<5	9.0	8.5	<8	7.5	7.5
35	6.0	<6	8.5	>8	7	7.5	<7
40	8.0	8.5	>7	7.5	>9	>10	9.5
45	9.0	10.0	8.5	8.5	14	>14	>14
50	>9	10.5	12.0	12.0	49= 15.0	47= 15.0	47= 15.0
55	9.0	>10	54= 15.0	15.0			
60	8.5	9.5					
65	>8	9.5					
70	>8>10						
75	9.5	11.5					
80	10.5	12.5					
85	>12	83− 15.0					
90	>14						
95	92− 15.0						

TDR	*Minutes to TDR*						
3	26	27	18	20	17	15	17
6	35	36	23	25	22	21	22
9	45	41	30	46	41	38	39
12	84	77	51	50	43	43	43

* These Runs Were Made During the Latter Part of the Program When Storage Instability Was Observed

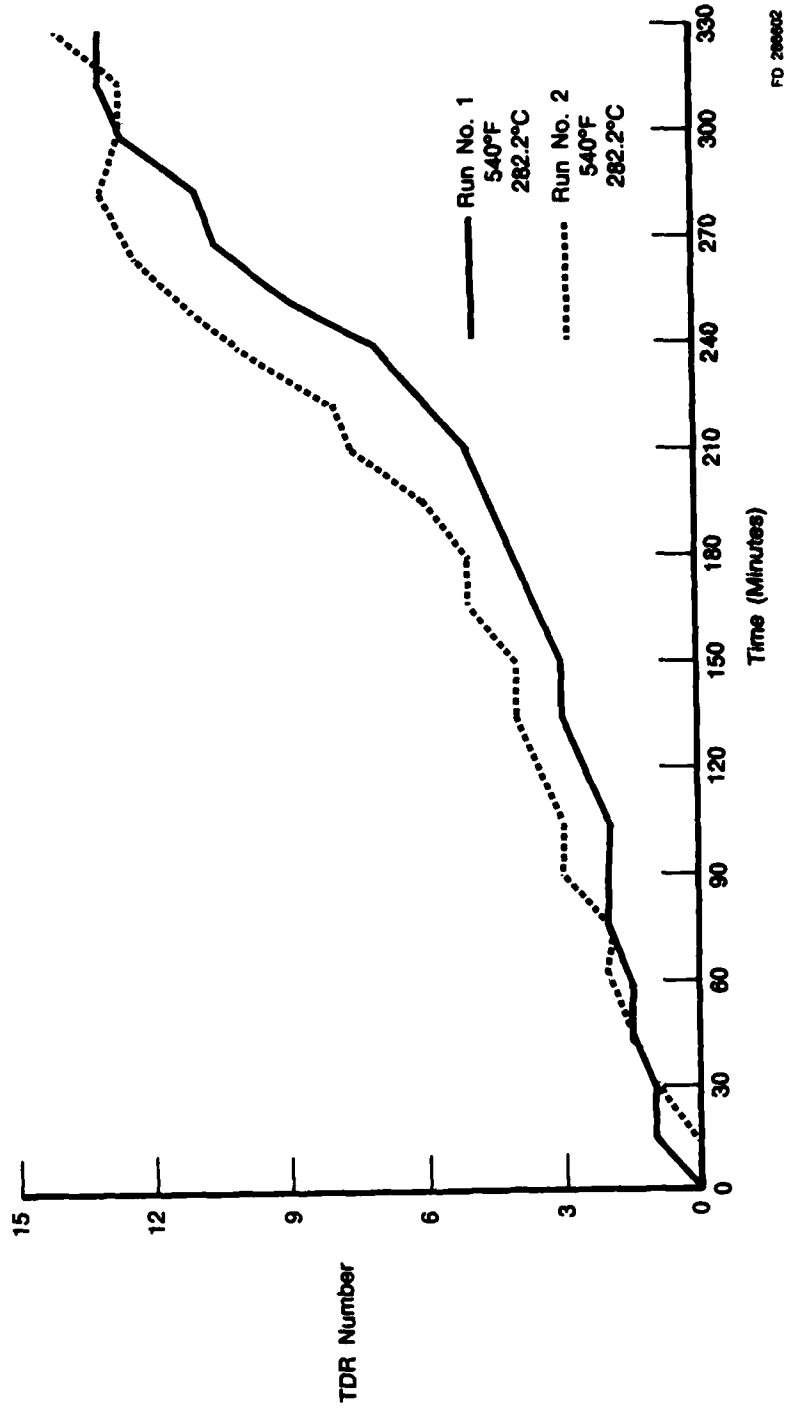

Figure II-4. Time to Attain TDR of 15.0 NAPC-5 Fuel

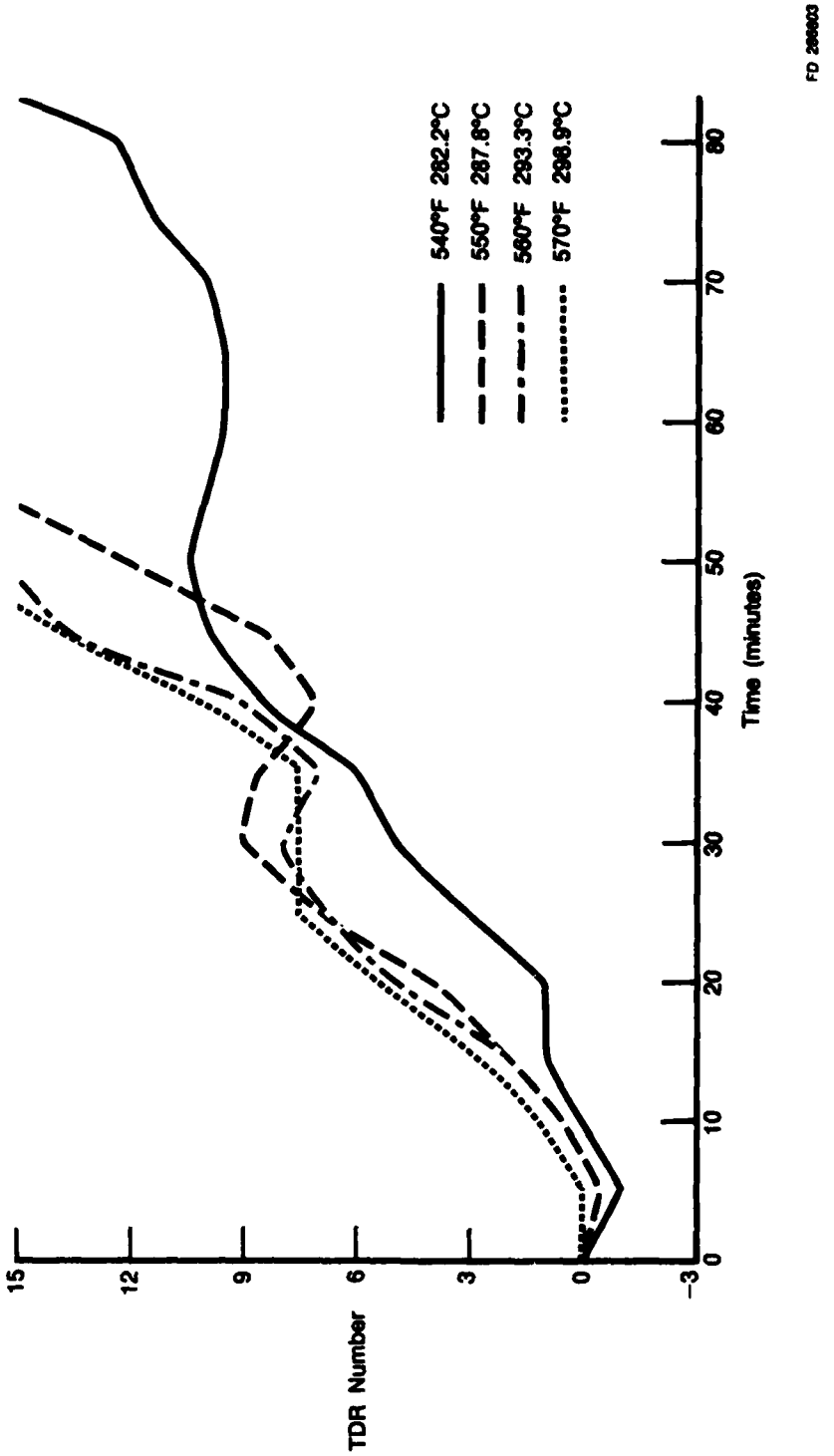

Figure II-5. Time to Attain TDR of 15.0 Temperature Profile: NAPC-5

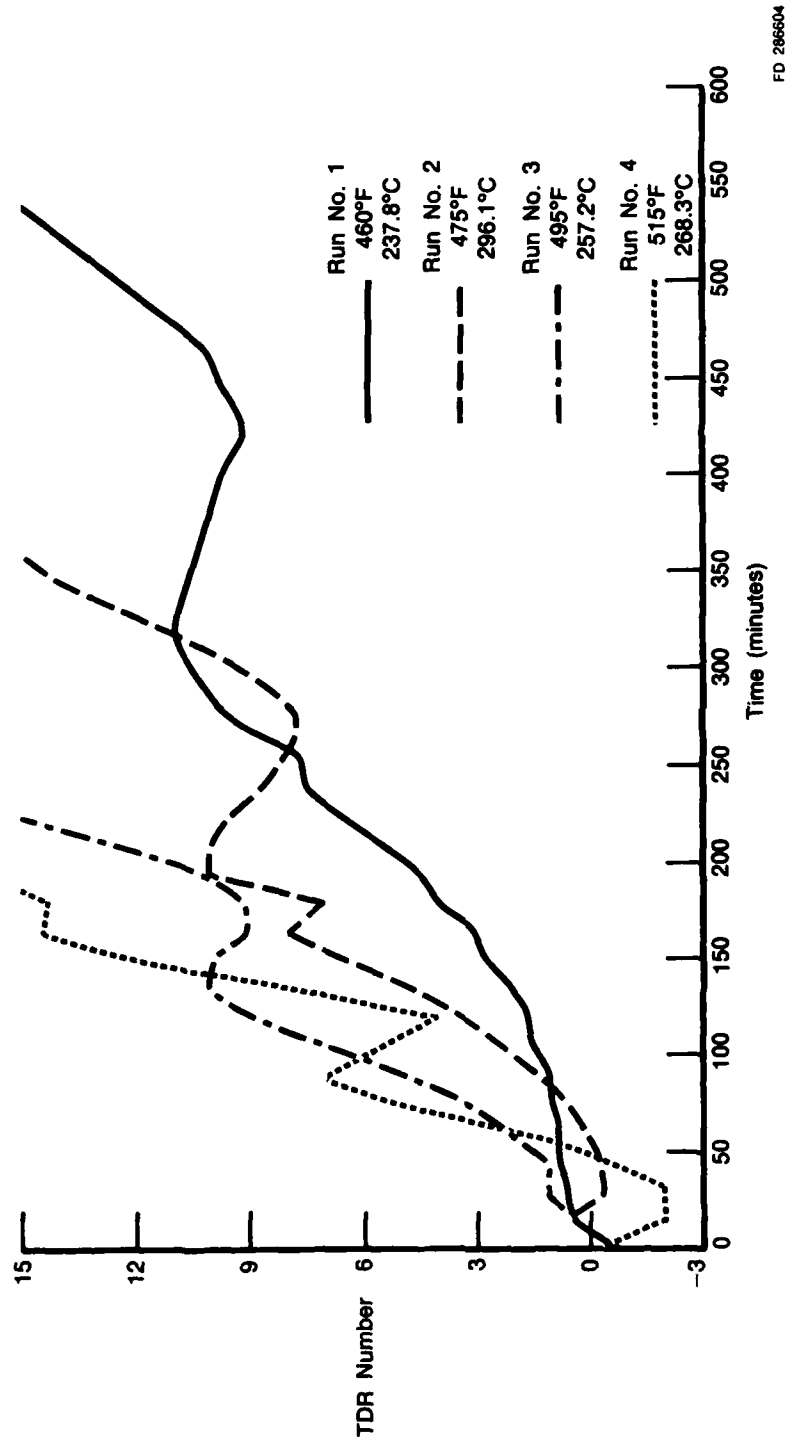

Figure II-6. Time to Attain TDR of 15.0 Temperature Profile: NAPC-7

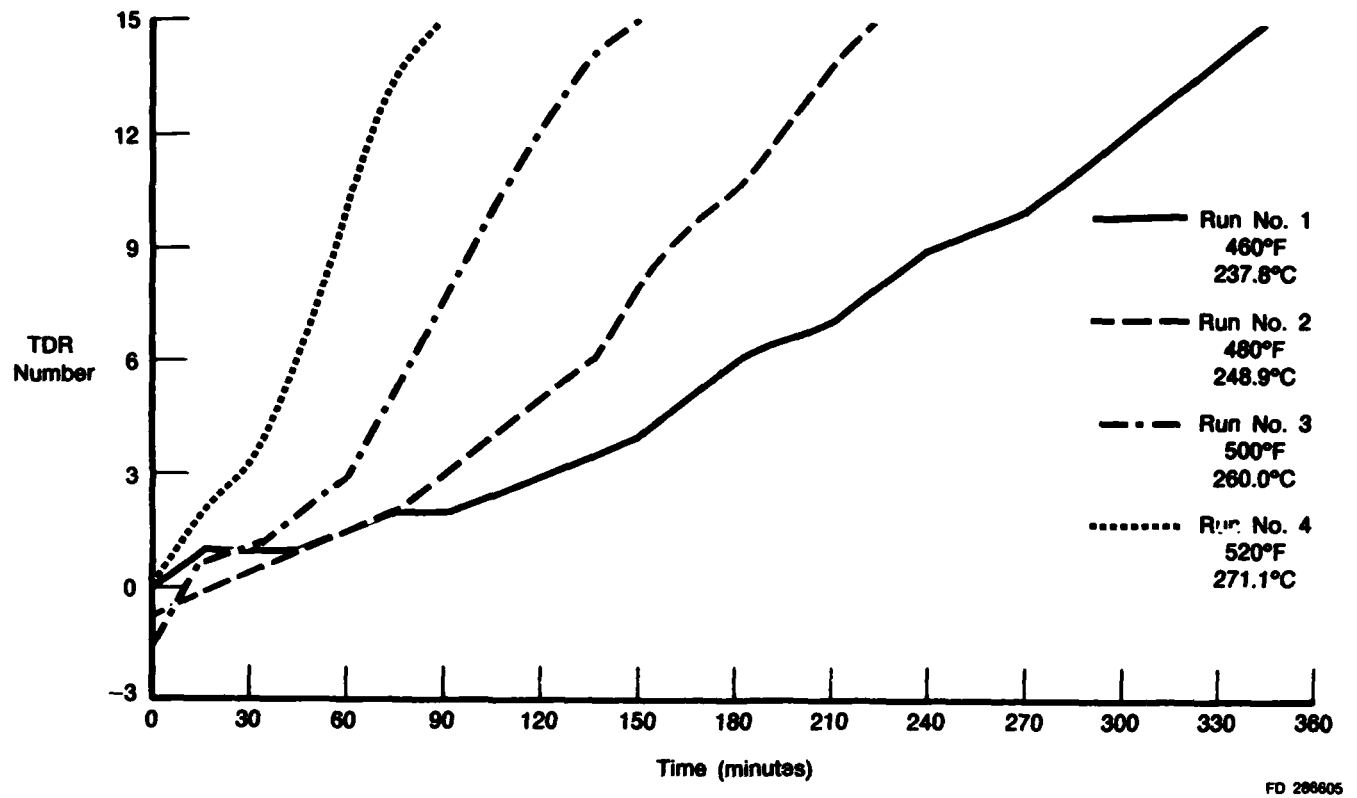

Figure II-7. Time to Attain TDR of 15.0 Temperature Profile: NAPC-11

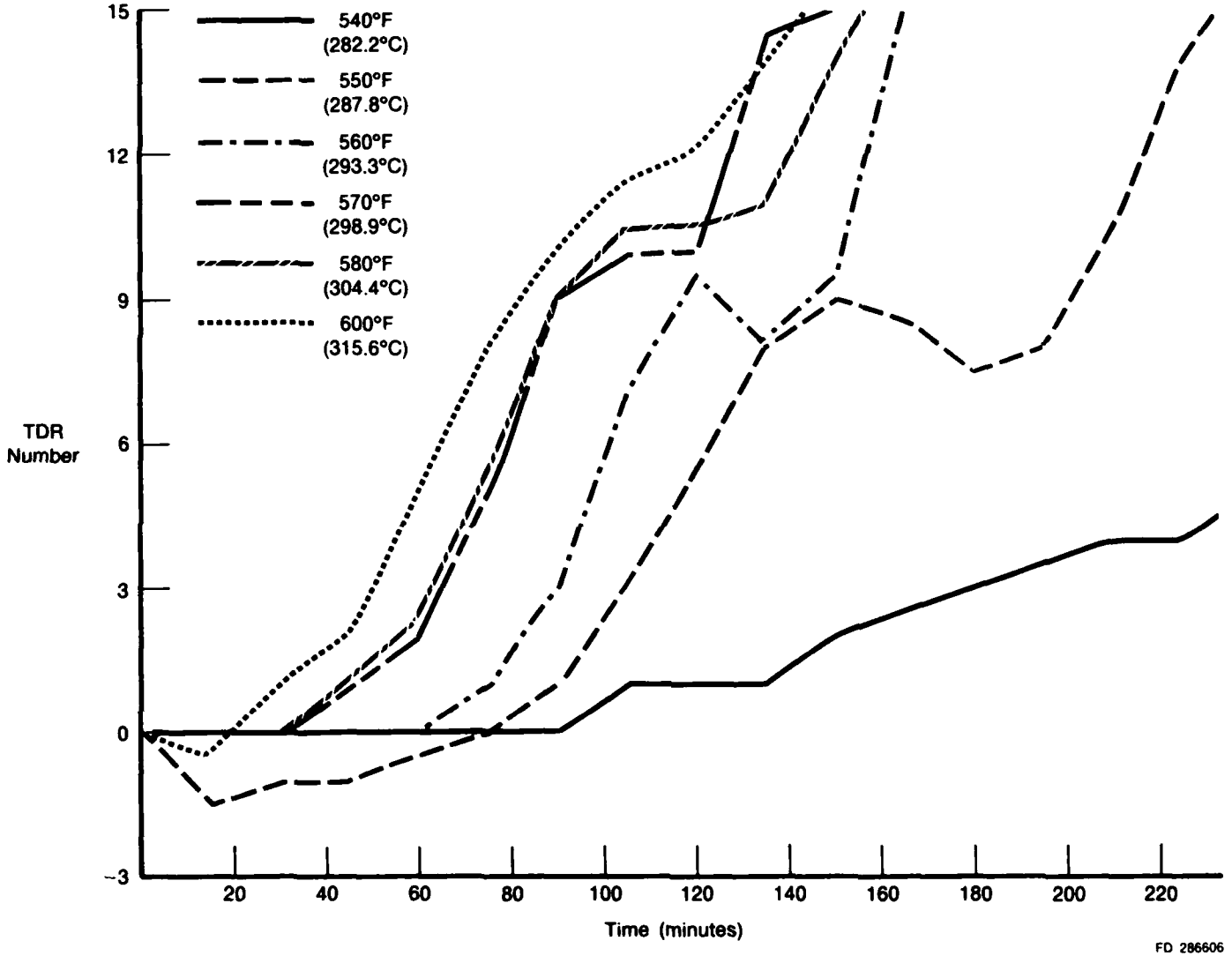

Figure II-8. Time to Attain TDR of 15.0 Temperature Profile: NAPC-14

Table II-5. Quartz-Enclosed Test Section JFTOT Runs Using Remote TDR Probe NAPC-5 Fuel

	Minutes Run Time to Attain TDR Readings				
Temperature, C (F)	*3.0*	*6.0*	*9.0*	*12.0*	*15.0*
271 (520)	—	—	—	—	—
277 (530)	115	145	—	—	—
277 (530)	26	35	45	84	92
282 (540)	27	36	41	77	83
282 (540)	150	225	255	295	—
282 (540)	123	150	210	—	—
288 (550)	18	23	30	51	54
288 (550)	20	25	46	50	55
293 (560)	17	22	41	43	49
293 (560)	106	—	—	—	—
299 (570)	15	21	38	43	47
299 (570)	17	22	39	43	47

Table II-6. Quartz-Enclosed Test Section JFTOT Runs Using Remote TDR Probe NAPC-7 Fuel

	Minutes Run Time to Attain TDR Readings				
Temperature, C (F)	*3.0*	*6.0*	*9.0*	*12.0*	*15.0*
238 (460)	165	218	270	497	543
238 (460)	182	235	330	527	591
246 (475)	117	146	191	325	360
246 (475)	120	147	178	320	345
257 (495)	77	103	122	207	226
257 (495)	77	106	135	220	240
268 (515)	65	82	144	150	187
268 (515)	63	78	102	153	167

Table II-7. Quartz-Enclosed Test Section JFTOT Runs Using Remote TDR Probe NAPC-11 Fuel

	Minutes Run Time to Attain TDR Readings				
Temperature, C (F)	*3.0*	*6.0*	*9.0*	*12.0*	*15.0*
238 (460)	120	183	242	300	354
249 (480)	88	132	161	193	230
249 (480)	80	125	153	184	219
260 (500)	58	81	100	118	160
260 (500)	60	84	105	127	153
260 (500)	50	85	107	126	154
271 (520)	30	47	57	68	87
271 (520)	37	54	70	81	97

Table II-8. Quartz-Enclosed Test Section JFTOT Runs Using Remote TDR Probe NAPC-14 Fuel

	Minutes Run Time to Attain TDR Readings				
Temperature, C (F)	*3.0*	*6.0*	*9.0*	*12.0*	*15.0*
271 (520)	300	490	760	1195	—
282 (540)	180	270	330	390	465
288 (550)	210	270	—	—	—
288 (550)	210	290	390	510	—
288 (550)	98	116	147	165	182
293 (560)	80	97	120	145	160
293 (560)	87	100	117	160	169
299 (570)	66	80	87	126	150
304 (580)	63	77	90	140	157
316 (600)	49	63	79	113	145

This conclusion was based on the smooth and continuous operation of the system as this TDR value was reached. Other higher TDR values were reached, but after delays or discontinuities.

In all tests conducted during this study, a point was reached at which the deposit (TDR) value would begin to decrease for a short, but specific, time. The TDR would then reverse, begin to increase, and continue to increase exponentially. In all cases, it appears that the TDR 6 would not be affected by these discontinuities or slope reversals. Higher TDR values, however, would be affected by the time interval between the first and second discontinuity. Earlier or lower TDR values would reflect variations in value due to early system instability or delayed deposition.

For Arrhenius calculations, 6 and 15 TDR values were used to determine the corresponding slope and resultant activation energy. Table II-9 lists, for each fuel, the Arrhenius parameters (activation energy and frequency factor) calculated from these two TDR values. The y-axis values were taken as the reciprocal of time in order to establish a negative slope by providing a TDR per time dimensional unit.

Table II-9. Arrhenius Parameters Based on the Time in Minutes to Reach TDRs of 6 and 15

	E^{*6}	A^{6}	E^{*15}	A^{15}
NAPC-5	15.4	3.6×10^{4}	19.6	6.8×10^{5}
NAPC-14	15.4	8.9×10^{3}	0.9	1.7×10^{1}
NAPC-7	18.3	3.2×10^{5}	20.2	8.4×10^{5}
NAPC-11	21.5	8.6×10^{6}	21.0	2.8×10^{6}

E* Values are Kilocalories Per Mole and Represent the Necessary and Sufficient Energy to Form Fuel Deposits
A Values are Per Second, and Represents the Degree of Order To Be Associated With a Hypothetical, High-Energy Fuel Deposit Precursor

Figures II-9 through II-16 show the experimentally developed Arrhenius plots for the four Navy fuels. Each plot represents a TDR value of 6 or 15. It is possible that several additional TDR values may be required to establish more specifically a constant TDR.

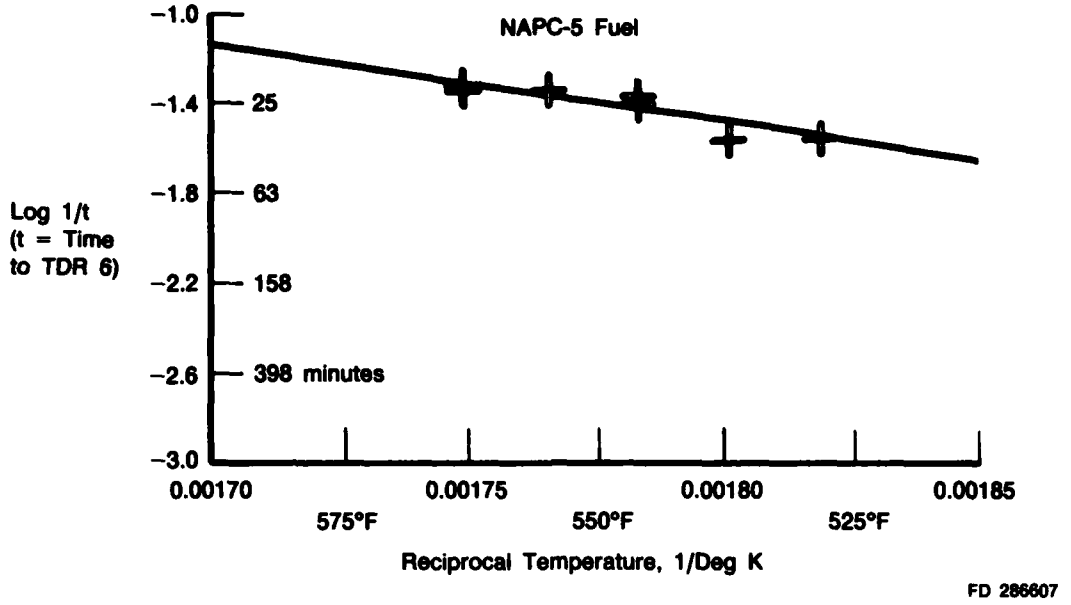

Figure II-9. Variation in Deposit Rate (TDR Time) With Fuel Temperature JFTOT — Time to Attain TDR of 6 NAPC-5 Fuel

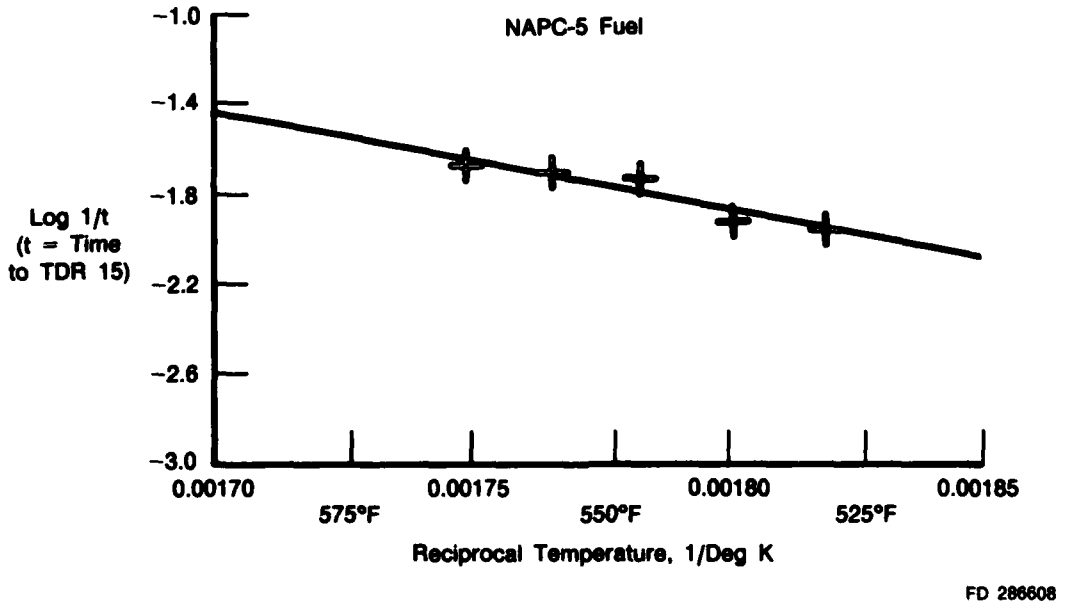

Figure II-10. Variation in Deposit Rate (TDR Time) With Fuel Temperature JFTOT — Time to Attain TDR of 15 NAPC-5 Fuel

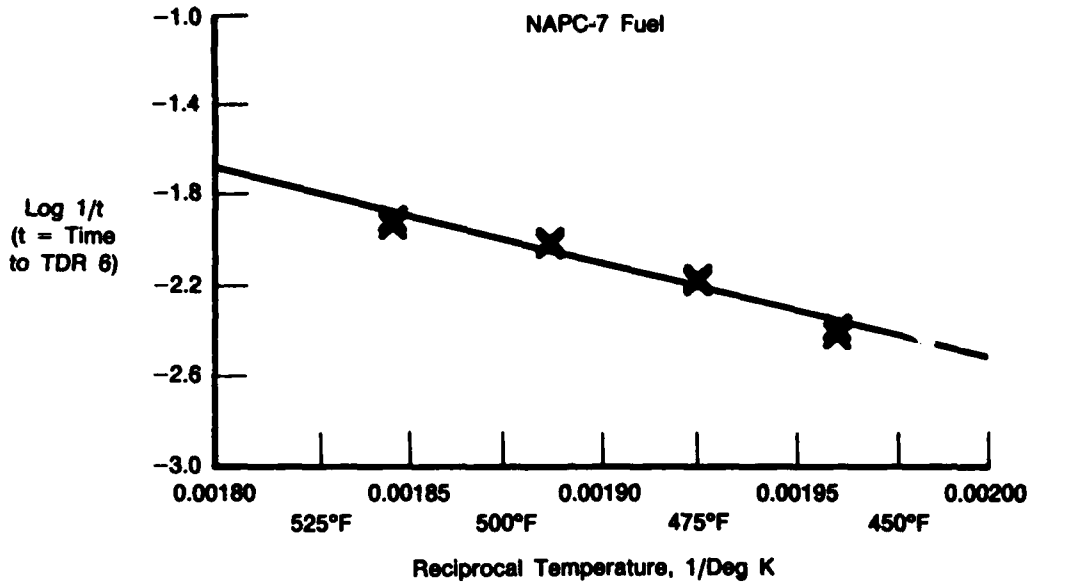

Figure II-11. Variation in Deposit Rate (TDR Time) With Fuel Temperature JFTOT — Time to Attain TDR of 6 NAPC-7 Fuel

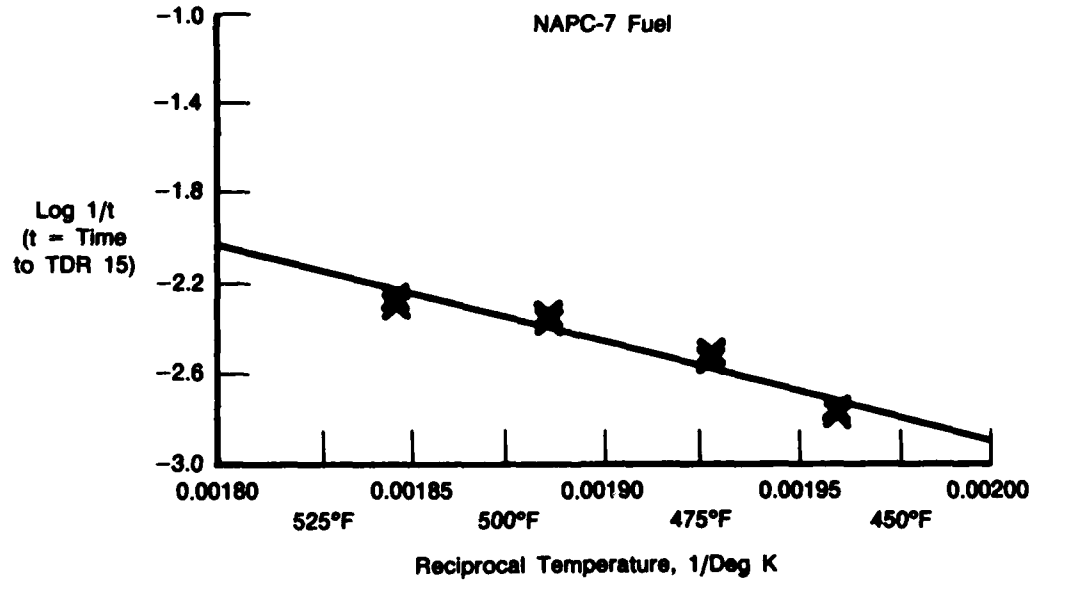

Figure II-12. Variation in Deposit Rate (TDR Time) With Fuel Temperature JFTOT — Time to Attain TDR of 15 NAPC-7 Fuel

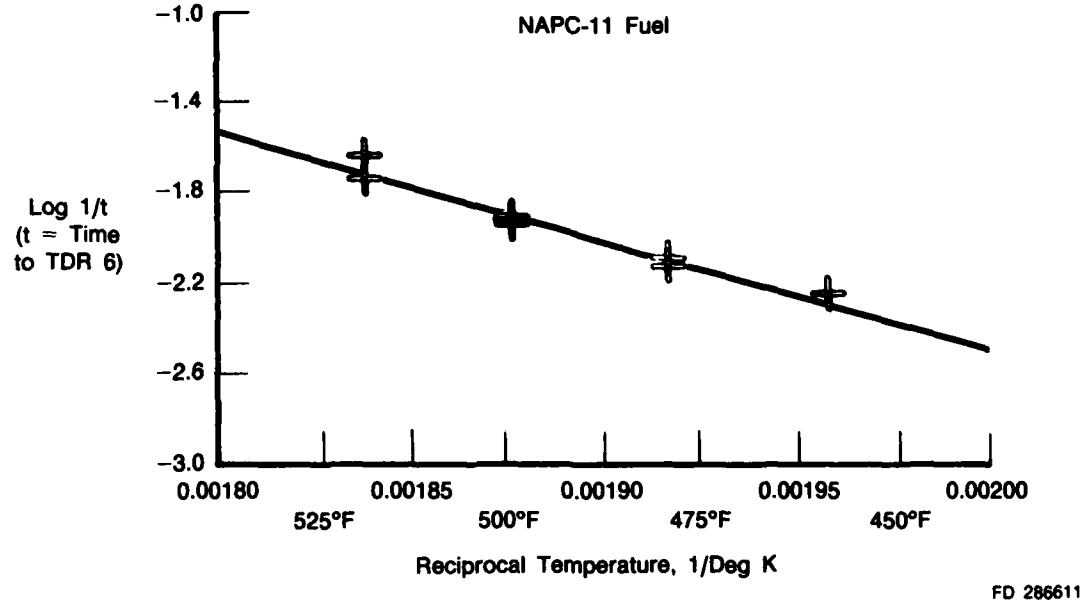

Figure II-13. Variation in Deposit Rate (TDR Time) With Fuel Temperature JFTOT — Time to Attain TDR of 6 NAPC-11 Fuel

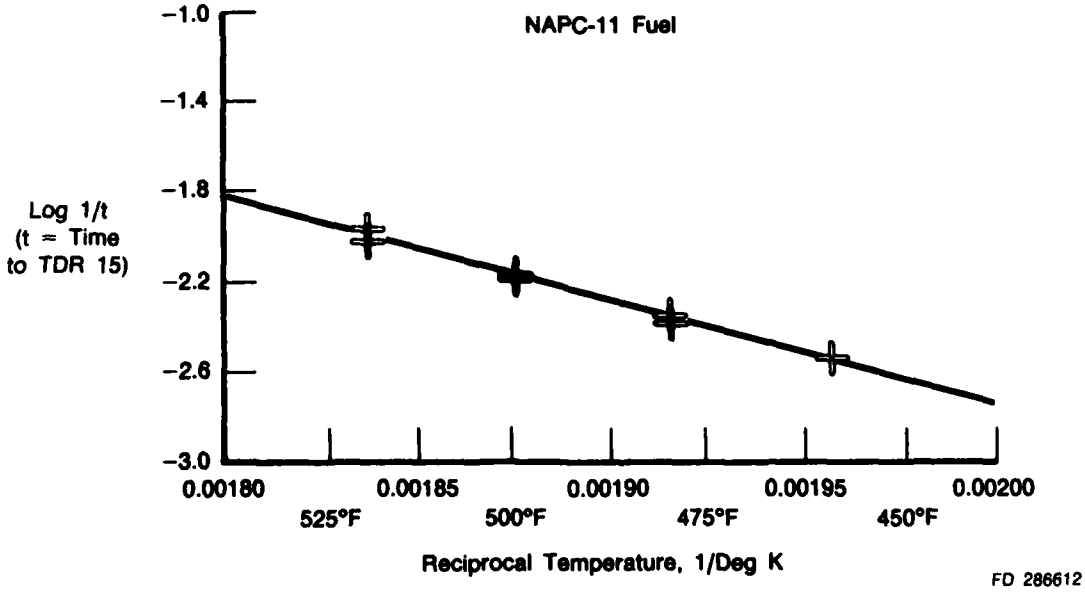

Figure II-14. Variation in Deposit Rate (TDR Time) With Fuel Temperature JFTOT — Time to Attain TDR of 15 NAPC-11 Fuel

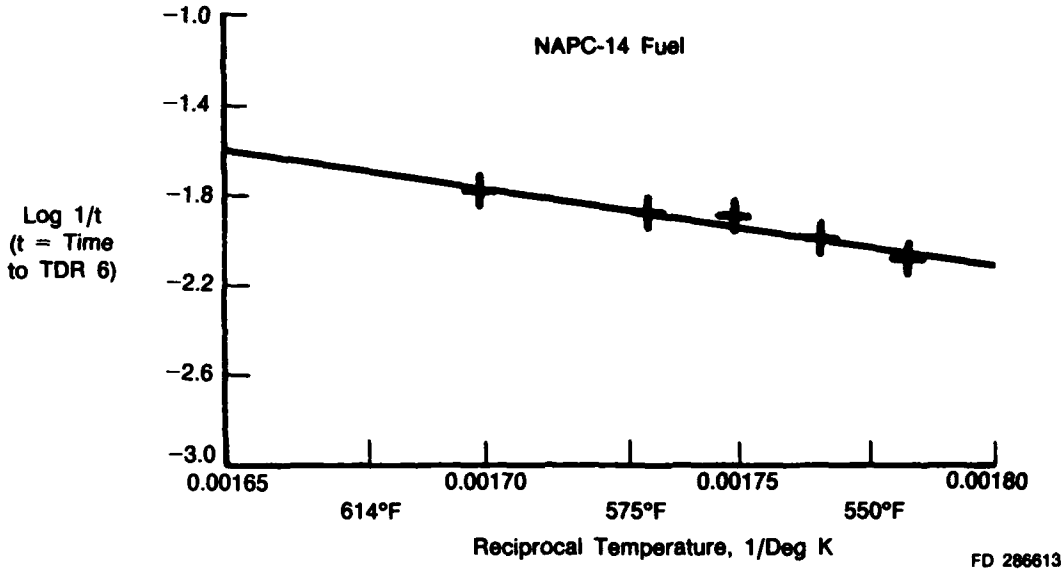

Figure II-15. Variation in Deposit Rate (TDR Time) With Fuel Temperature JFTOT — Time to Attain TDR of 6 NAPC-14 Fuel

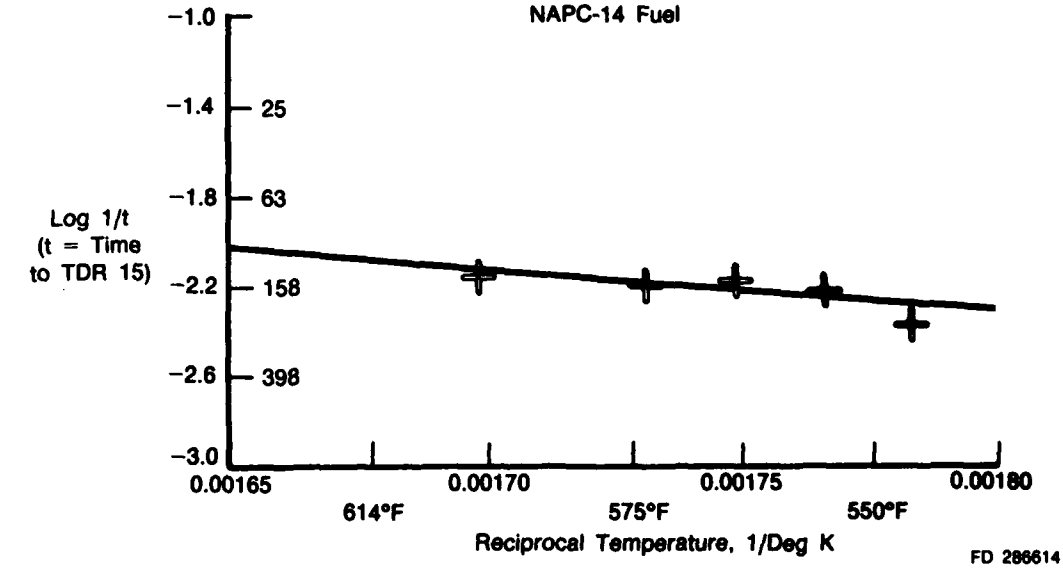

Figure II-16. Variation in Deposit Rate (TDR Time) With Fuel Temperature JFTOT — Time to Attain TDR of 15 NAPC-14 Fuel

C. JFTOT PEROXIDE ANALYSIS

During the testing conducted with the modified JFTOT, samples of fuel were analyzed for organic peroxides using ASTM D-3703-78. Peroxides have been associated with the chemical mechanisms proposed by many investigators as intrinsic to the autoxidation of hydrocarbon

fuels. It has been suggested that the thermal instability of hydrocarbon-derived fuels is related directly to the hydroperoxide formation rate. The specific rate of formation of these fuel-produced peroxides was sought in order to develop a valid fuel peroxide/fuel deposition relationship and to extend the relation to include the fuel thermal breakpoint temperatures.

Several alternate designs were made to modify the JFTOT fuel system downstream of the differential fuel filter; however, the 500-pound-per-square-inch fuel pressure made impossible the removal of the necessary fuel sample for peroxide analysis. Removal of even small fuel samples would disrupt the JFTOT flow and, thereby, void the test.

A fuel sampling system was designed and fabricated to sample the stressed fuel for peroxide analysis. The apparatus consisted of a small, pressurized reservoir, with a 100-mL capacity and appropriate 1/8 inch stainless fuel lines and stainless valving. The effluent fuel from the hot test section was diverted to the inlet port of the small reservoir and through the top exit port to the fuel/water heat exchanger. The following procedure used for collecting the stressed fuel samples. The 100-mL collecting reservoir was filled with the test fuel, sealed and plumbed into the JFTOT test section hardware. The collecting reservoir was equipped with a magnetic stirring device which was set at approximately 300 rpm. The base fuel in the reservoir is displaced as the effluent from the hot test section is admitted to the bottom entrance port of the collecting reservoir. In actual practice, the effluent fuel at a given temperature is pumped through the collecting system for 60 minutes at 3.0 mL/minute.

The collecting reservoir is removed from the system by sequencing the appropriate valves and directing the spent test fuel directly to the heat exchanger. This method of collecting fuel samples for peroxide number evaluation was tried a number of times. Apparently, the fuel present in the reservoir prior to the test cycle is never completely displaced by the hot test fuel.

Another method of sample collection was to sample the test fuel directly from the spent fuel discharged to the standard 1.L reservoir. The JFTOT fuel lines, heat exchanger and pump were thoroughly rinsed with the fuel to be analyzed. Prior to the start of the test cycles, the fuel was allowed to flow through the entire system for one to two hours. The fuel reservoir was then cleaned and filled with pre-filtered fuel, and the test fuel aerated before reservoir assembly.

The JFTOT was then run at the desired temperature for one hour and shut down hot. The hot shutdown precluded the admission of any non-stressed fuel to the fuel aliquot that was to be analyzed for peroxide number. The test fuel, ~180 mL, was decanted from the reservoir to a beaker and its test temperature was identified. The floating piston and lip seal of the reservoir assembly provided a leak-proof barrier to prevent dilution of the spent fuel by the fresh fuel below the piston.

The reservoir was then sealed again, and a new test was started at a higher temperature. Temperatures were elevated in 20°F increments as listed in Table II-10. These sequential tests, involving shutdown and startup every 60 minutes, were used instead of a complete run at one temperature. This approach minimized any variables which would have resulted from the use of different aliquots of fuel for different temperatures.

Peroxide concentrations were found to vary in an arbitrary manner based on previous thermal stress testing and concurrent ECA tests. After testing fuel samples from NAPC-5 and NAPC-7, it was concluded that no meaningful peroxide data would be forthcoming from the modified JFTOT remote probe tests. At the conclusion of the unsuccessful JFTOT peroxide tests, a sample of each fuel was thermally stressed at 100°C for a period of time necessary to demonstrate the nature (level) of the fuel's peroxide potential. This was done in accordance with ASTM D-3707 as modified by the Peroxide Potential Panel, Jet Fuel Thermal Stability of the CRC. Table II-11 lists the data resulting from these tests.

Table II-10. Peroxide Concentration of Fuel as a Function of Thermal Stressing by JFTOT*

Fuel Stress Temperature, C (F)	Fuel			
	NAPC-5	NAPC-7	NAPC-11	NAPC-14
25 (77)	3.90	Trace	BDL**	1.12
227 (440)	7.57	1.44	BDL	2.29
238 (460)	11.75	2.02	BDL	2.36
249 (480)	16.77	2.18	BDL	4.42
260 (500)	20.51	2.18	BDL	6.62
271 (520)	21.12	2.92	BDL	10.32
282 (540)	19.74	5.00	1.06	14.42
293 (560)	19.06	9.58	BDL	15.87

* Concentration in Parts Per Million
** Below Detectable Limits

Table II-11. Peroxide Concentration[f] Increase as a Function of Residence Time at 100°C (212°F)

Time, Hours	NAPC-5	NAPC-7	NAPC-11	NAPC-14
0	3.90	Trace	BDL[e]	1.12
48	81.34	3.55	BDL	27.46
72	228.80	6.89	3.98	61.48
96	243.08	8.40	3.06	162.28
168	197.05	10.12	BDL	151.20
192	208.38	12.69	BDL	119.52
216	236.04	17.94	BDL	100.16
240	245.94	21.00	BDL	105.26
264	246.69[a]	31.33	BDL	84.64
360	257.35[b]	215.66[c]	BDL	48.18
384	242.54	400.15	BDL	55.08[d]
408	179.40	545.74	BDL	35.34
432 (18 days)	135.26	627.25	BDL	37.30

[a] Peroxide Concentration 271.06 When Using 10 mL Rather Than 25 mL Freon 113. Peroxide Concentration 277.51 When Using 10-Minute Reaction Time Rather Than the Specified 5-Minute Reaction Time

[b] Peroxide Concentration 275.32 When Using 10-Minute Reaction Time. Peroxide Concentration 292.81 When Using 20-Minute Reaction Time

[c] Peroxide Concentration 232.15 When Using 10 mL Freon 113. Peroxide Concentration 232.52 When Using 10-Minute Reaction Time

[d] Peroxide Concentration 63.21 When Using 10-Minute Reaction Time. Peroxide Concentration 73.02 When Using 20-Minute Reaction Time

[e] BDL — Below Detectable Limits

[f] Peroxide Concentration in Parts Per Million

D. ECA TESTS

The ECA, which was designed, fabricated and tested in the fuel laboratory at P&W/GPD, has been described elsewhere.[1] Appendix A outlines the system as it was used in this program. The basic assumption of the test methods of the ECA is to avoid any possible influence of oxygen concentration on the rate of fuel deposition. In order to accomplish this, the ECA has been designed to maintain the concentration of oxygen at a constant level. In this study, standard air with an oxygen concentration of 21% (volume) was the preselected level in all ECA tests. This level was found, in previous tests, to be acceptable with a one-hour test duration.

All four fuels were evaluated at test fuel temperatures from 138°C (280°F) up to 288°C (550°F) in 50-degree increments. Test pressures were varied based on the critical pressure. Table II-12 lists the test pressures used for each fuel based on the pseudo-critical pressure established by Kay[2].

Table II-12. Critical Test Properties of Navy Fuels

	NAPC-5	*NAPC-7*	*NAPC-11*	*NAPC-14*
Boiling Point (Mean), °C	216	230	243	207
Breakpoint (JFTOT), °C	271-282	246	243	271
Gravity (API)	40.8	35.7	39.7	43.7
Critical Pressure (MPa)	2.30	2.31	2.04	2.30
ECA Test Pressure	2.50	2.50	2.30	2.50

The mean boiling point for each fuel was derived, according to Maxwell[3], from the atmospheric distillation of a 100-ml sample of each fuel. The 10, 50 and 90% temperatures were used to determine an average boiling point.

The API gravity and these average boiling points were subsequently used to establish the pseudo-critical pressure. The pseudo-pressure for each fuel was increased by 30% to establish the working test pressure for ECA tests up to 290°C.

There were no major problems encountered with the ECA tests conducted with any fuel in this program.

ECA test data for each Navy fuel is listed in Table II-13. Data at the 138°C test temperature was not available because the one-hour test duration was not long enough to produce repeatable deposition. Selected data from the ECA tests were repeated to verify the validity of specific reaction rates. For the NAPC-5, −7 and −11, data at 150°C and 235°C were repeated, and for NAPC-14 the 288°C test temperature was repeated. Repeat data was within 10% of the original test point. Temperature and specific deposition rates are also listed in Table II-13. Figure II-17 is a composite plot of all four Navy fuels and allows an easy comparison of the ECA deposition rate data and their slopes and linearity.

[1] Pratt & Whitney Final Report Contract F33615-82-C-2210 currently in process and CRC Thermal Stability Conference presentation, of 30 April 1980, entitled: "Thermal Stability of Jet Fuels: A Preliminary Study of the Kinetics of Coke Formation from Jet Fuels".
[2] Kay, W.B., Indust. Engr. Chem., Vol. 32, No. 3, 1940, pp. 353-7.
[3] Maxwell, J.B., *Data Book on Hydrocarbons*, 1902, 1st Edition, p. 72.

Table II-13. Navy Fuel Thermal Deposition Data

NAPC Fuel Type	Fuel Temperature °C	Fuel Pressure psi	Specific Rate of Fuel Deposition grams/cm² hour
5	137	365	—
14	139	361	—
7	138	375	—
11	137	336	—
5	151	367	2.76×10^{-4}
14	152	365	6.99×10^{-4}
7	149	374	1.1178×10^{-3}
11	154	335	1.911×10^{-3}
5	176	371	5.72×10^{-4}
14	178	362	1.285×10^{-3}
7	177	376	3.186×10^{-3}
11	176	337	3.989×10^{-3}
5	208	362	7.42×10^{-4}
14	205	371	3.062×10^{-3}
7	207	375	8.412×10^{-3}
11	206	331	8.752×10^{-3}
5	236	363	1.168×10^{-3}
14	231	370	8.983×10^{-3}
7	233	376	1.0622×10^{-2}
11	234	330	2.6215×10^{-2}
5	260	363	2.553×10^{-3}
14	264	362	2.1817×10^{-2}
7	259	374	2.6349×10^{-2}
11	261	331	3.7456×10^{-2}
5	287	368	2.741×10^{-3}
14	283	367	2.7221×10^{-2}
7	284	376	3.3224×10^{-2}
11	286	332	7.0982×10^{-2}

Arrhenius activation energies were calculated from the data given in Table II-9. The manner of deriving the activation energy was unique to the type of data based on fuel deposition. The total temperature dependency[1] of a fuel's autoxidation mechanism is difficult to define mathematically. The principle reason is that most petroleum or shale-derived fuels do not have a single, specific mechanism that can be characterized as governing the overall autoxidation process. Instead, the choice of specific reaction limits is needed to define the activation energy. However, even with the most limited system, the preexponential factor remains uncharacterized.

[1] Total temperature dependency, as applied here, means both the Arrhenius activation energy and the Arrhenius preexponential factor

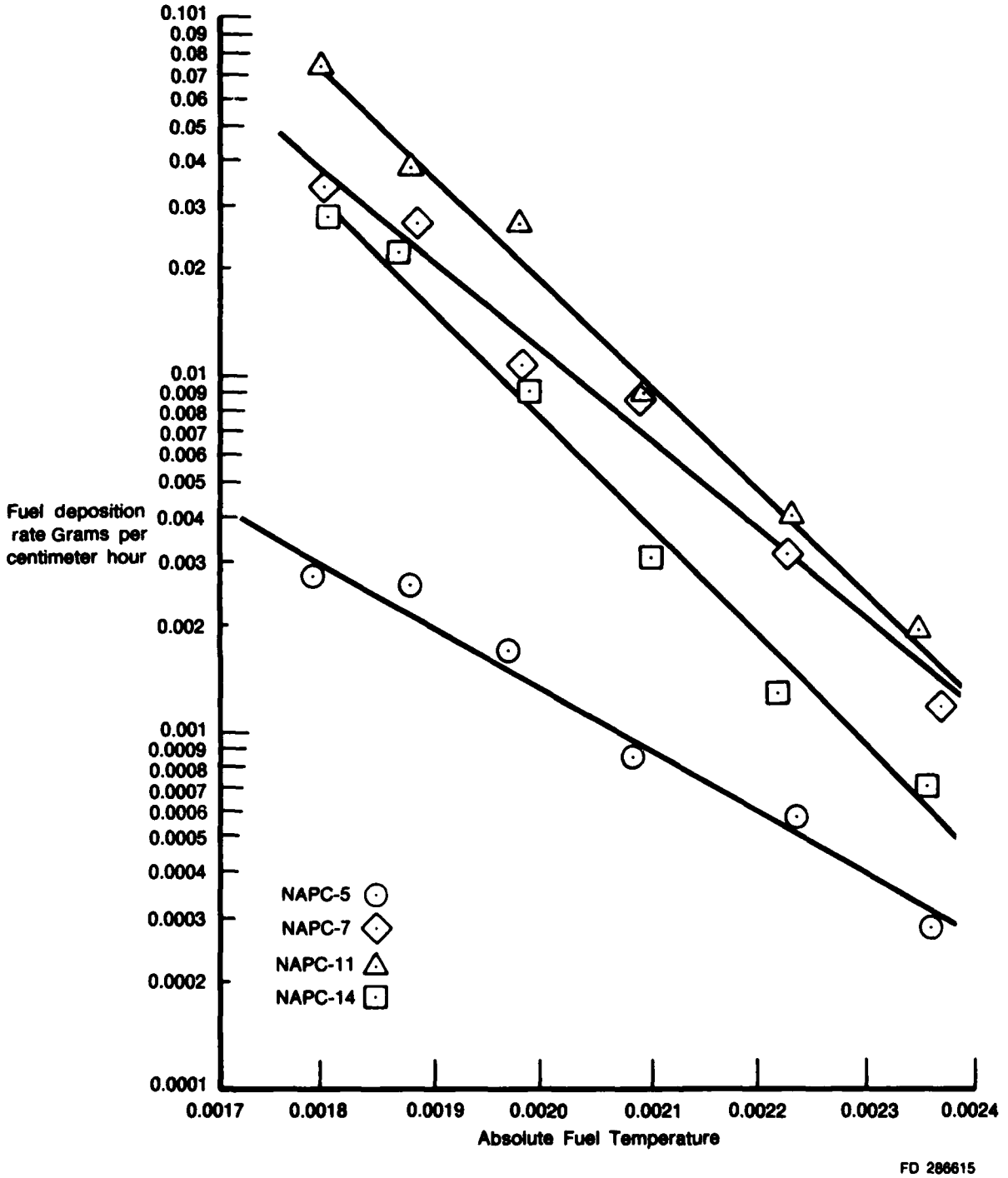

Figure II-17. Navy Fuel Deposition Rate Expressed as the Variation of the Specific Deposition Rate as a Function of Temperature

Calculated Arrhenius activation energies and the coefficient of determination are tabulated in Table II-14. Data in this table are for the JFTOT remote probe tests and the ECA tests. The JFTOT data is tabulated for TDR numbers of 3, 6, 9, 12 and 15. This was done initially to compare the ECA activation energies to the various TDR energies and, based on this comparison, to allow the recommendation of a standard TDR. Comparisons were made, but no definitive result was established because the activation energies were not comparable for different fuels and their equivalent ECA energies. For this reason, the previously described TDR standard development was undertaken and the resultant standard TDR of 9 was established.

Table II-14. Activation Energy for NAPC Fuels at Various TDR and From the Experimental Coking Apparatus

	NAPC-5		*NAPC-7*		*NAPC-11*		*NAPC-14*	
TDR	*Each*	r^2	*Each*	r^2	*Each*	r^2	*Each*	r^2
3	15,499	0.807	20,405	0.950	19,012	0.843	18,153	0.991
6	15,357	0.760	18,280	0.969	22,243	0.974	16,005	0.980
9	3,162	—	15,727	0.824	22,705	0.969	14,184	0.934
12	19,983	0.841	21,541	0.983	22,794	0.976	15,430	0.992
15	19,562	0.844	10,957	0.696	22,085	0.987	11,563	0.889
				ECA Data				
	8,287	0.961	11,668	0.980	13,096	0.991	14,122	0.984

From Table II-14, the calculated activation energies can be compared. It should be noted that, except for the NAPC-14 fuel, the TDR derived energies are higher by 8 to 10 kilocalories than the ECA values. These values are very close to each other.

Associated with the Arrhenius activation energies are the coefficients of determination represented in Table II-14 by r^2. These values relate the relative goodness of the linear curve fit of the deposition data. Data from ECA tests show a very high coefficient, while data from the JFTOT tests vary over a much broader range (i.e., ± 0.015 for the ECA compared to ± 0.150 for the JFTOT).

SECTION III
CONCLUSIONS AND RECOMMENDATIONS

A. CONCLUSIONS

In addition to the general conclusions described in the technical section, several additional results are noteworthy.

The overall performance and repeatability of the Jet Fuel Thermal Oxidation Tester (JFTOT)/remote probe method to determine the intrinsic fuel deposition rate is excellent. The theory, application and resulting data from this method are comparable and, in some cases, superior to currently existing systems. The only limitation to this JFTOT approach is the relatively low quantity of molecular or dissolved oxygen available for the oxidation to occur. The oxygen in the JFTOT studies is limited to 50 to 100 millimoles, and, as a result, the overall reaction rate expression would be second-order. The Experimental Coking Apparatus (ECA) which results in a pseudo-first-order rate, can be used to supplement the JFTOT data and resultant Arrhenius parameters by eliminating the oxygen effect on the deposition specific rate.

From the breakpoint temperatures, established to within 5.5 °C, the thermal stability of the four NAPC fuels was initially found to be in order of decreasing stability:

NPAC-5~NPAC-14>NAPC-7>NAPC-11

NAPC-5 and NAPC-14 were found to have approximately the same breakpoints, with NAPC-7 and NAPC-11 measurably lower (i.e. 271-282, 271, 246 and 243°C respectively). The variation in breakpoint for NAPC-5 is understandable because of its intrinsic storage stability variation.

The Arrhenius activation energies for the four fuels were of the same order with regard to increasing energy as were the previously stated breakpoints with regard to a decrease in test temperature. This is valid only with the TDR of 6. The TDR of 15 data does not follow a specific pattern due primarily to the fact that the two points of inflection have partially distorted the deposition kinetics.

In order to establish the peroxide potential for the fuels used in this study, all four fuels were thermally stressed at 100°C for the times shown in Table II-11. Several conclusions can be suggested from these data. First, the higher breakpoint fuels were NAPC-5 and NPAC-14. These two fuels formed a significant peroxide concentration in a very short time (48 hours) relative to the other two fuels. NAPC-7 required over 275 hours at 100°C to reach this same level, and NAPC-11 never reached more than 4 parts per million of peroxide. These data indicate the following order of decreasing peroxide potential:

JP-5(Petroleum),JP-5(shale),80%JP-5+20THCGO,50%JP-5+50%HCGO

Secondly, the hydrocracked gas oil (HCGO) improved or decreased the peroxide potential at 100°C. Data established from the JFTOT remote probe tests also indicated the order of thermal, deposition-derived activation energies

JP-5(Petroleum)≈JP-5(shale),80%JP-5+20%HCGO,50%JP-5+50%HCGO

in the order of increasing energy.

Both during testing and at the conclusion of the technical effort with the modified JFTOT, a series of data comparisons were completed. These comparisons were done in order to define potential relationships between a measured fuel property and one of the new remote probe JFTOT properties (e.g. breakpoint versus time to TDR-6). It was found that, with high breakpoint fuels, the time to TDR was shorter than with a low breakpoint fuel. This conclusion should be used in a limited way because there were only three fuels and limited breakpoints. (The fourth, NAPC-5, showed variation under storage conditions.) Although these data are inconclusive, it was established that there is a potentially sound relationship between the breakpoint temperature and the deposit as measured by the remote probe (TDR). Future tests should provide additional data to support the relationship.

B. RECOMMENDATIONS

Additional testing of the JFTOT remote probe system is recommended in order to determine the following:

1. Heater tube material effects on the rate of fuel deposition

2. The necessary conditions for a single TDR to be used for development of Arrhenius data from a broader range of gas turbine fuels

3. The applicability of this method for reduced pressure (200-400 psi) fuel system deposition

4. Additive effects, both single and synergistic, on the overall thermal stability of jet fuels

5. Effect of a longer heater tube section (up to 5 inches) with two remote probes located 180 degrees apart

6. Modification of the photodetector so that specific deposit materials can be evaluated.

These data could be used to establish an additional thermal stability criteria to supplement and possibly replace the visual-coded JFTOT measurements.

Peroxide measurements should be made only after the current ASTM procedure has been modified to obtain more repeatable information. The very nature of peroxide instability necessitates a marked improvement of this procedure before any realistic Arrhenius data can be generated from peroxide analysis.

APPENDIX A
THEORY AND OPERATION OF THE EXPERIMENTAL COKING APPARATUS

The Experimental Coking Apparatus (ECA) was initially designed to study the rates of jet fuel deposits found in the mechanical fuel systems aboard gas turbine powered aircraft. It is basically a stainless steel, 2-liter, cylindrical reaction chamber which contains the necessary material and induction coil to heat a sample of jet fuel to any prescribed temperature inductively from ambient to 340°C.

The ECA was used throughout this program to establish gravimetrically the maximum amount of deposit that can be realized from a prescribed volume of fuel. The experimental test conditions were as follows:

1. The test temperature is in the range characteristic to auto-oxidation from ambient to 288°C. For the purposes of this study, the minimum temperature was taken as 121 to 135°C. Both chromel/alumel and platinum/platinum-rhodium thermocouples were used to measure test temperatures;

2. Test pressures were recorded on both helicoil pressure gages and digital readouts using Teledyne™ transducers. The test pressures were set according to the pseudo-critical pressures as discussed in the body of this report.

3. Standardized, compressed air cylinders were used to supply a steady, continuous flow of oxygen into the base of the reaction chamber of the ECA. The flow rate was 300 standard cubic centimeters per minute measured continuously at a downstream location by a Matheson Model 8240 mass flow controller. The kinetic analyses and Arrhenius evaluations that are used to relate fuel deposit characteristics to the changes in fuel composition based on a first-order rate mechanism were the only concentration variables in the fuel component. This air flow is of utmost importance because of the necessity to provide a very high concentration of oxygen compared to the amount of fuel components that will produce fuel deposits at the test condition.

4. The duration of each ECA test was established by measuring the time necessary to condense a gravimetrically determinable fuel deposit on a 4-square-inch coupon. For the selected fuels in this study, a 60-minute test duration at temperature was used; however, three to four hours was necessary for JP-7 to provide a measurable deposit.

The ECA is shown in Figure A-1 in schematic form. During the tests conducted with the fuel baseline and blend tasks, the following modified test procedure was used. The reaction chamber was manually filled with one liter of fuel to be tested. This amount of fuel covered both the susceptor and the induction coil. The induction heater leads, which are located inside the reaction chamber, are coated with a composite material that has no effect on the thermal or chemical stability of jet fuels at elevated temperatures and pressures. These leads were also covered with fuel. After the fuel had been added, two sample coupons of stainless steel were placed into the sample holder as shown in Figure A-2. The platinum thermocouples were placed into the susceptor, and the sample holder was placed in the top of the reaction chamber. A visual inspection was made prior to each test from the top of the ECA. After it was confirmed that the coil, susceptor and sample coupons were all in their proper places, the top was positioned with an

ATC-AES 1002-2 AGC Fluorocarbon Elastomer Gasket. The nitrogen system was activated to 207 kPa, the reaction chamber was pressure checked for leaks, and the pressure was reduced to atmospheric. This completed the pretest setup and checkout.

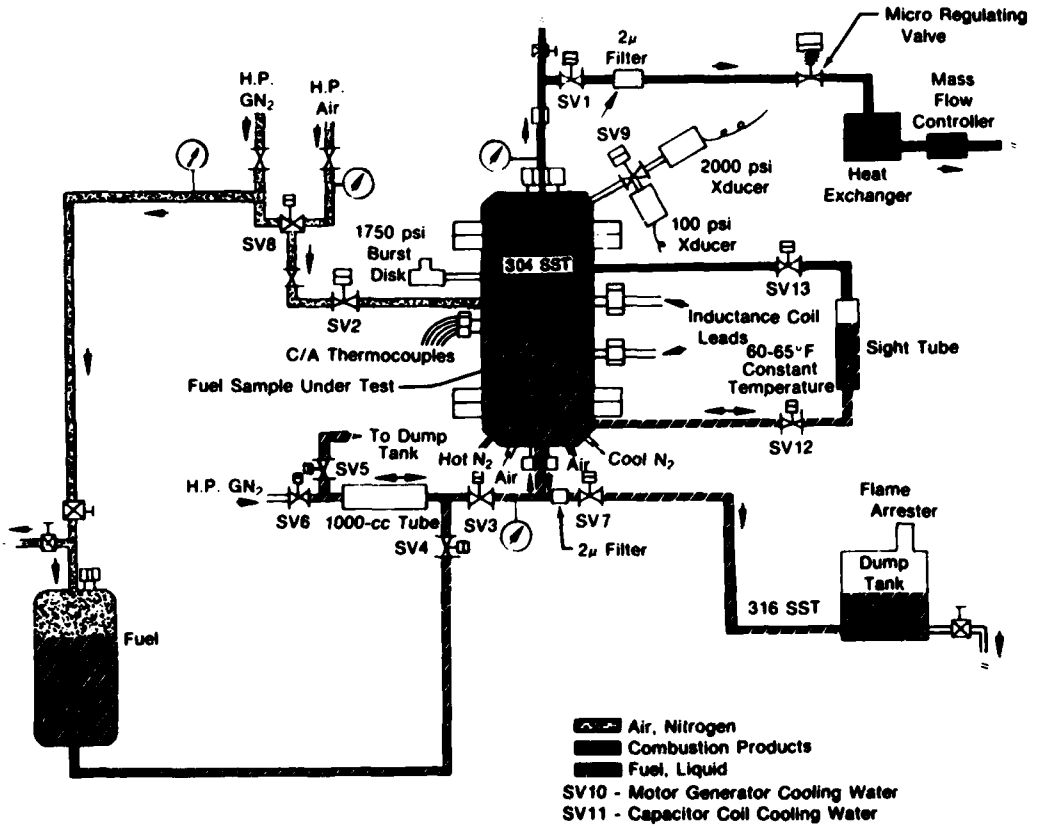

Figure A-1. Schematic of Experimental Coking Apparatus

The 15-kilowatt Tocco induction heater was then brought on line in accordance with the manufacturer's instructions, and the temperature of the susceptor was increased from ambient to 38°C. The susceptor was held at this temperature for one minute to activate the Leeds and Northrop Model 165 temperature controller. Next, the high-pressure regulated air supply was activated, and the reaction chamber pressure was brought to 10% above the psuedo-critical pressure. After a stable pressure was established, the Matheson mass flow controller was turned on and a flowrate of 300 SCCM of dry standard air was maintained during the remainder of the test. With both the pressure and flowrate set and constant, the induction heater was turned to full power, and, simultaneously, control was transferred to the temperature controller. The Leeds and Northrop controller not only controlled the maximum test temperature but also controlled the rate of heating or the variation of temperature flux to the fuel from the susceptor. A timer on the Tocco control unit was set to the required run time after the test temperature had been reached.

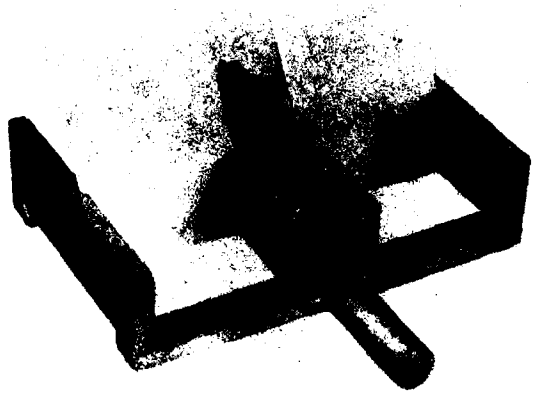

FE 355302

Figure A-2. Sample Coupons Mounted in Holder

At the conclusion of each test, the reaction chamber was allowed to cool for one hour at ambient pressure and at 300 SCCM of nitrogen as a system purge. The sample coupons, shown in Figure A-3, were removed from the sample holder, washed with a solution of hexane and toluene, and placed in a vacuum oven at 100°C for one hour at a pressure of five inches of mercury. After the initial drying period, one sample coupon was labeled and placed into an amber or brown jar, covered with a nitrogen blanket and sealed for shipment to Wright-Patterson Air Force Base. The other coupon was weighted on a Mettler Model M5SA six place to within one microgram. The coupon was then cleaned with a proprietary multiple-solvent to remove all deposit material, and the coupon reweighted. This gravimetric differential was used as the basis for the specific deposit rate for the test fuel. Figure A-4 shows a series of sample coupons from tests run from 121 to 288°C in 28° increments. Both the baseline and fuel blend deposition rates were established as described; refer to Appendix C.

Fuel samples for the peroxide analyses (as described in Appendix B) were taken immediately at the conclusion of the preset time at temperature. A 75-gram sample of fuel was withdrawn, under pressure, into a nitrogen purged borosilicate glass sample bottle. The sample was divided into at least three separate samples, and each sample was analyzed for the level of peroxide in parts per million in accordance with ASTM D-3703-78.

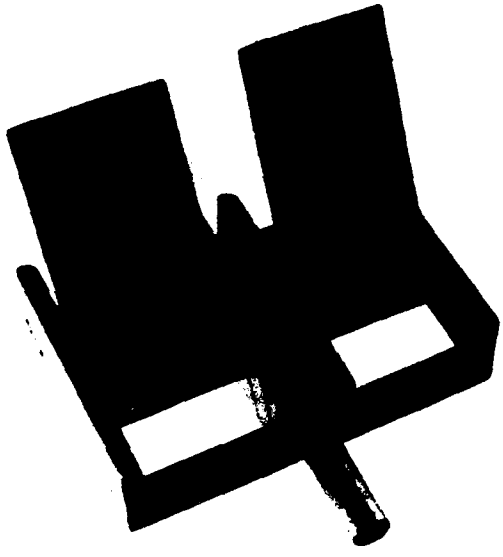

FE 356291

Figure A-3. Sample Coupons Removed from Holder and Washed

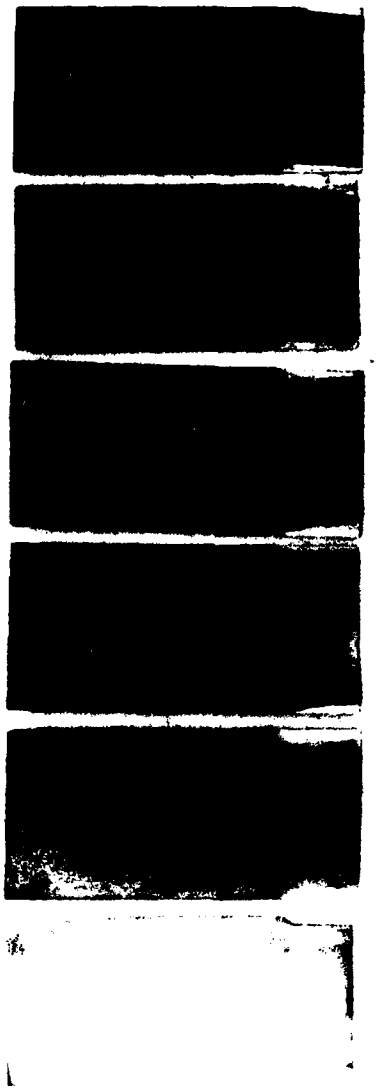

FE 356293

Figure A-4. Sample Coupons Tested at Temperatures from 21 to 288°C

APPENDIX B
A TEST METHOD FOR THE DETERMINATION OF THE PART-PER-MILLION LEVEL OF ACTIVE OXYGEN IN AVIATION TURBINE FUELS

The products of auto-oxidation of gas turbine fuels contain substantial and measurable quantities of oxygen in addition to other elements. Chemical mechanisms have been proposed that treat the chemical reactions responsible for incorporation of molecular oxygen int The procedure that follows was used explicitly to determine the part-per-million level of peroxide in fuel samples. The samples evaluated by this method were analyzed immediately after thermal stressing had been completed on the Experimental Coking Apparatus (ECA). Fuel samples were not held overnight nor refrigerated due to potential continuation of possible peroxy free radical reactions.

This method is a modification of the ASTM D3703-78, a standard test method for evaluating the peroxide number of aviation turbine fuels. All requests used in these determinations are described in this ASTM procedure.

A sample of fuel to be tested was divided into three aliquoits and measured gravimetrically to ± 0.002 gram. The sample was immediately sparged with pure, dry nitrogen gas. The sparging was carried out in a 250-ml iodine flask for samples with a peroxide cor tration of 75 ppm or more, while a 500-ml iodine flask was used for concentrations less than 75 . The iodine flasks and all other equipment that came into contact with the fuel sample had been final rinsed with pure ethyl alcohol just prior to use to remove any trace quantities of moisture. The iodine flask also were flushed with pure, dry nitrogen just prior to introduction of the fuel sample.

After the sample was sparged for a minimum of three minutes at at rate of 200 SCC, 25 ml of Freon 113 was added, and the sparging was continued for a minimum of five minutes. A stirring motor using a magnetic stir bar was used to agitate the solution vigorously after the Freon 113 was added to the fuel sample. Without stopping the sparging, 20 ml of Ultrex acetic acid was added followed by two to three ml of freshly prepared/stabilized potassium iodide.

The use of the terminology, stabilized, may be misleading when used without explanation. In thee analyses, the potassium iodide was prepared freshly on a daily basis as follows: First, 50 ml of deionized water was filtered (0.8 micron) and sparged vigorously with pure, dry nitrogen for three minutes, while the temperature was increased to 90°C. Then, 75 grams of ACS reagent grade potassium iodide was slowly added and magnetically stirred until the iodide was completely dissolved. Finally, the solution was cooled to room temperature and topped off with nitrogen. Every effort was made to ensure a less than detectable amount of free iodine would be formed through complete exclusion of molecular oxygen.

After the potassium iodide had been added, the nitrogen flow was increased to 500 SCCM and held there for 30 seconds. The nitrogen flow was terminated, and the flask was set aside for 5 minutes ± 3 seconds. During this time, the peroxides present in the original fuel sample reacted and oxidized iodide ion to free iodine which was then titrated with a standard sodium thiosulfate as described in Section 8.3 of ASTM 3703:78. The resultant calculations of parts-per-million were converted into both millimoles of active oxygen[1] per liter of fuel and millequivalents of active oxygen per kilogram of fuel. Figure B-1 shows various chemical apparatus used in these analyses, and Table B-1 lists the specific chemicals.

---

[1] Active oxygen is defined as one-half of the oxygen of a fuel-derived hydroperoxide. Millequivalent weight of 8.

FBC 46066-3

Figure B-1. Chemical Apparatus Used During Analyses

Table B-1. Peroxide Analysis Equipment/Materials

Burets, Fisher Brand Machlett Automatic Burets

$Na_2S_2O_3$	*Capacity*	*Subdivision*	*Tolerance*	*Reservoir Capacity*	*Cat. No.*
0.1N	2ml	1/100ml	± 0.02ml	500ml	03-847A
0.01N	10ml	5/100ml	± 0.06ml	1000ml	03-847D
0.005N	25ml	1/10ml	± 0.06ml	2000ml	03-847E
Freon 113	25ml	1/10ml	± 0.06ml	2000ml	03-847E

NOTE: Filters, Plugs, and Silica Gel Come With Burets.

Fisher Support Assembly for Machlett Burets, Rectangular Cast Iron Support

Model, 14-679

This Stand Is for One Buret Only. Included Are, Clamps and Ring Supports.

Fisher Scientific Co.

Graduated Cylinder With Stopper. Cat. No. 08-565D

Fisher Scientific Co.

Pyrex Brand Flask - 250ml, Cat. No. 10-094B
Stopper No. 14-640-3.

Fisher Scientific Co.

Kimax Brand Flask, 500ml, Cat. No. 10-096C

Fisher Scientific Co.

Kimax Brand, 25ml, Cat. No. 10-100B. Stopper No. 16.

VWR Scientific Inc. Borosilicate Glass Pasteur Pipets.

Length 5-3/4 in. Cat. No. 14673-010
Length 9 in. Cat. No. 14673-043

VWR Scientific Inc. Disposable Pasteur Pipets.

Length 5-3/4 in. Cat. No. 14672-200
Length 9 in. Cat. No. 14672-380

Fisher Scientific Co.

Corning Magnetic Stirrers, Model - PC353-14-511-200.

VWR Scientific Inc., Stir Bars, Magnetic, Star Head Nalgene.

Height × Diameter = 5/16 × 3/8 in., Nalge No., 6600-00-10, Cat. No., 58958-502
Height × Diameter = 9/16 × 3/8 in., Nalge No., 6600-00-14, Cat. No., 58948-513.

Fisher Scientific Co., Kimax Brand, Reusable Glass Culture Tubes.

OD × L
25 × 150, Cat. No. 14-930-10J
Screw Caps, GCMI Size, 24-410, Cat. No. 14-930-15J.
Blue, Epoxy Coated Rack, 28 cm × 21 cm × 10 cm, Cat. No. 14-793-4.

Fisher Scientific Co.

Balance-Mettler, PC Series, Model PC 220.

Matherson

Regulator-Model No., 3104.

Fisher Scientific Co., Racon 113, Freon.

Trichloro-1,2,2, Trifluoroethane.

APPENDIX C
JET FUEL THERMAL OXIDATION TESTER

Appendix C contains information directly concerned with the use of the Inter Av Research Jet Fuel Thermal Oxidation Tester (JFTOT) with a visual heater tube section and a remote probe/TDR deposit measurement system. Paragraph A describes the methods used to prepare for the JFTOT test, paragraph B describes the test procedure that was used for all tests in this investigation, and paragraph C describes the method for establishing the linearity between the strip chart recorder and the modified Mark VIII A Tuberator, and paragraph D lists the apparatus and tools necessary for this type of test.

A. PREPARATION FOR TEST

The following procedures were used to prepare for the JFTOT test.

1. Calibration of heater tube temperature controller is accomplished by strict adherence to Section 6.2 of ASTM D-3241 procedure as specified in the 1983 ASTM Annual Book of Standards.

2. Inspection of component parts of JFTOT of TOFT is accomplished by strict adherence to Sections 6.3 and 6.4 of the ASTM D-3241 procedure. The quartz tube is inspected for any signs of craze and replaced as required.

3. Cleaning of reservoir, fuel lines and pre-filter assembly is accomplished as specified by Section 6.5, paragraphs 6.5.1 through 6.5.11, of the ASTM D-3241 procedure, except the components are air dried from a compresses air cylinder rather than a squeeze bulb.

4. Assembly and installation of pre-filter is accomplished by strict adherence to Section 6.7 of the ASTM D-3241 procedure. ASTM D-3241 states: "This procedure is valid when using either a 1L or a 3L fuel reservoir."

5. Preparation of test fuel is accomplished by strict adherence to Section 6.8 of ASTM D-3241 procedure with the exception of paragraph 6.8.2. As a result of this exception, the specified 600 mL of fuel is changed to "required volume of fuel needed for projected length of test cycle".

6. Assembly of reservoir system is accomplished by strict adherence to Section 6.9, paragraphs 6.9.1 through 6.9.10, of the ASTM D-3241 procedure. This assembly procedure is valid for 1L or 3L reservoir.

7. Pre-calibration of heater tube is accomplished in the following manner. The heater tube is rated before testing, both visually and by the light reflectance method, using the Mark VIII A Tuberator. The tube is rated in 4-mm increments from the 12-mm position to the 54-mm position. For the purpose of this program, two sets of readings were taken by the light reflectance method. The Spun reading was taken on all zones and recorded. Then each zone was rated by the Spot method with the highest Spot reading at each zone being recorded on the data sheet as High, Spot and pre Test.

8. Cleaning and assembly of heater tube test section is accomplished in the following manner. The quartz tube with mating Viton A O rings is

positioned between the two end plates of the GLTS-102 test section, and the end plates are tightened into position. The test section is thoroughly cleaned with isooctane and air dried. The ID of the quartz tube is cleaned with ethyl alcohol and a nylon brush and air dried.

The assembly of heater tube and filter into the quartz-enclosed test section is accomplished in accordance with Section 6.6, paragraphs 1 through 9, of the ASTM D-3241 procedure.

9. Installation of test section into JFTOT is accomplished by strict adherence to Section 6, paragraphs 6.6.10 through 6.6.17, of the ASTM D-3241 procedure.

B. TEST PROCEDURE

The following procedures were used for all tests in this investigation.

1. Fuel system pressurization is accomplished by strict adherence to Section 7, paragraphs, 7.1.1. through 7.1.18, of the ASTM D-3241 procedure.

2. Setting of controls is accomplished as stipulated in Section 7.2, paragraphs 7.2.1 through 7.2.9, of the ASTM D-3241 procedure with the following exception. Paragraph 7.2.3 should be amended to read: "The timer can be electrically bypassed to allow a test run time of any length without interrupting the test cycle."

   An alternate method of running longer than the five-hour cycle is to momentarily depress the heater switch which will automatically reset the timer to another five-hour cycle.

3. The SKAN-102[1] remote probe is attached to the support rods of the glass preheater section and positioned with the probe pickup slit even with the 38.7-mm zone of the preheater tube. This positioning is accomplished by previously scribing a reference mark on each of the two support rods.

   The probe is not positioned until the fuel system has been pressurized, flow rate established and test section checked for leaks. The quartz outer tube is thoroughly cleaned using Chem Wipes™ saturated with ethyl alcohol and is dried by rubbing with dry Chem Wipes.

4. With the correct operating pressure and fuel flow rate established at ambient temperature, the Mark VIII A Tuberator indicating needle is set at 0 by means of the Lo Cal adjustment knob. The strip chart recorder is set at 10-MV sensitivity and the chart speed set at 4 inches per hour. If the recorder pen is not on the preselected zero position, an adjustment can be made with the recorder zero control.

5. The test section heater switch is turned to the desired wattage for the selected run temperature. When the test section heater is energized, an immediate negative deflection of the TDR Meter needle and the recorder

[1] SKAN-102 is a cadmium sulfide photodetector resistor with a visual light range of 550 mm (±50%).

pen will be observed. No adjustments to the meter or recorder are to be made.

6. When the preselected test temperature is reached, the filter differential pressure system is activated and, if required, adjusted to zero.

7. As the run progresses, the negative deflection of the TDR an recorder will decrease with a zero meter and recorder reading occuring usually during the first 30 minutes of the heated test cycle. It is a desirable practice during the early part of the test to periodically check the TDR and recorder to assure linearity between the two instruments. With linearity assured, observations need be made only to check operating conditions and possible pressure drop across the test filter.

8. The thermal stability run is terminated when the desired tube deposit rating is observed. The test section heater is turned off and pressure drop, if any, is recorded. Fuel flow is continued through the test section for ~ 5 minutes to lower the test section temperature to ~ 125°F.

9. The fuel pump is shut off, the fuel system pressurization valve is closed, the differential pressure measurement system is bypassed,and the system vent valve is opened to bleed system at ~ 0.15 MPa/s, (22 psi/s).

10. When the system pressure reaches zero, the testing hardware is dismantled. The preheater is to be held only by the shank ends to avoid all contact with the tube area that contacts fuel.

11. The preheater tube is flushed with isooctane and air dried with clean compressed air. The heater tube is replaced in the original container, and the tube container is identified by appropriate wording.

12. Heater tube deposit rating is accomplished by strict adherence to Section 9 of the ASTM D-3241 procedure as specified in the 1983 ASTM Annual Book of Standards.

SPOT deposit rating of the preheater tube can be facilitated by marking a position on the rotation knob for reference. A drop of Liquid Paper has been found to be adequate to identify an easily seen reference point.

C. ESTABLISHMENT OF LINEARITY BETWEEN STIP CHART RECORDER AND MODIFIED MARK VIII A TUBE DEPOSIT RATER

1. Introduction

During this program, it was decided to further modify the Mark VIII A Tuberator by the addition of suitable pickup receptacles attached to a strip chart recorder. The recorder receptacles pick up their signal from the output going to the indicating needle of the Mark VIII A. The advantage of the recorder is that the Mark VIII A does not have to be continually monitored to observe deposit buildup versus run time. Also, at the end of each test run, there is a graphical record of deposit buildup as a function of time.

2. Linearity Procedure

The following procedures are used to establish linearity between the strip chart recorder and the Mark VIII A.

1. Clamp SKAN-102, Remote Probe, to quartz test section complete with polished unused preheater tube.

2. Turn TDR power switch to ON position, and switch two way toggle switch to Remote Probe position. (Allow 5 minutes warmup time before use.)

3. Turn recorder switch to ON, sensitivity to 10 mV, and chart speed to 4 inches per hours.

4. Move indicating needle of Mark VIII A to 0 by means of the Lo Cal control.

5. Move recorder pen to desired zero position on chart by means of the recorder zero adjust knob.[1]

6. Make a recorder trace of sufficient length; recorder chart speed can be increased to 4 inches per minute for this purpose, to ensure that the zero TDR meter reading remains at the zero position on the recorder. Minute adjustments of meter and recorder may be required at this time.

7. When all zero adjustments are made, raise the TDR meter reading to 5 by means of the Lo Cal adjustment knob.

8. Adjust the recorder SPAN to the desired SPAN range by using the recorder SPAN adjust knob. P&W four small recorder divisions (10 mm) for each single number of the TDR meter. Run a trace, as in step 6, to ensure true linearity at the TDR meter reading of 5. Repeat these steps for meter readings of 10 and 15.

9. As a final check for linearity, make short recorder traces at TDR readings of 0, 5, 10, and 15.

D. APPARATUS AND ASSOCIATED EQUIPMENT USED FOR QUARTZ TEST SECTION PROGRAM

The following apparatus associated equipment were used for the quartz test section program.

1. TOFT, Model 260, Thermal Oxidation Fouling Tester — ALCOR Inc.

2. TOFT, Model 360, Thermal Oxidation Fouling Tester — INTER AV Inc.[1]

3. TUBERATOR, Model Mark VII A, Modified, ALCOR Inc.

4. VISUAL TUBERATOR, Model VTR-100, ALCOR Inc.

5. REMOTE TDR PROBE, Model SKAN-102, INTER AV Inc.

[1] A standard JFTOT, ALCOR Inc., is suitable for this test procedure.

6. QUARTZ ENCLOSED TEST SECTION, Model GLTS-102, INTER AV Inc.

7. STRIP CHART RECORDER, HEWLETT PACKARD, Model 7132A or Equivalent[1]

8. REPLACEMENT QUARTZ TUBES , 0.500 inch ± 0.003 inch O.D., 0.197 inch ± 0.002 inch ID, by 37 mm long. INTER AV Inc.

9. HEATER TUBE AND FILTER KIT, Ref. No. JFT-100, ALCOR Inc.

10. BORE BRUSH, No. 915AB-4 or equivalent, Meriam Instrument Co.

11. ISOOCTANE, REAGENT GRADE, FISHER SCIENTIFIC Co.

12. EHTYL ALCOHOL, U.S. INDUSTRIAL CHEMICAL Co.

13. CLEAN, DRY, HYDROCARBON FREE supply of compressed air (Linde Air Products, Size A cylinders have proved satisfactory.)

14. Two stage air regulator capable of 30 psi discharge pressure through 1/4 inch OD flexible line

15. Fuel pressurization system, standard nitrogen cylinder with regulator to pressurize the system to 3.45 MPa (500 psig).

[1] During this program, Hewlett Packard 9280-0264-1 chart paper was used for recording purposes. This paper is marked with ten major increments of 25 mm per division. Each major increment has 10 minor divisions spaced at 2.5 mm. The zero chart position used was the first major line 25 mm from the left of the paper. This positioning left adequate room to quantify the negative deflection of the recorder pen as units of a TDR number. By selecting 10 mV sensitivity for the recorder, each TDR number increase was equivalent to four small divisions (10 mm) on the chart.

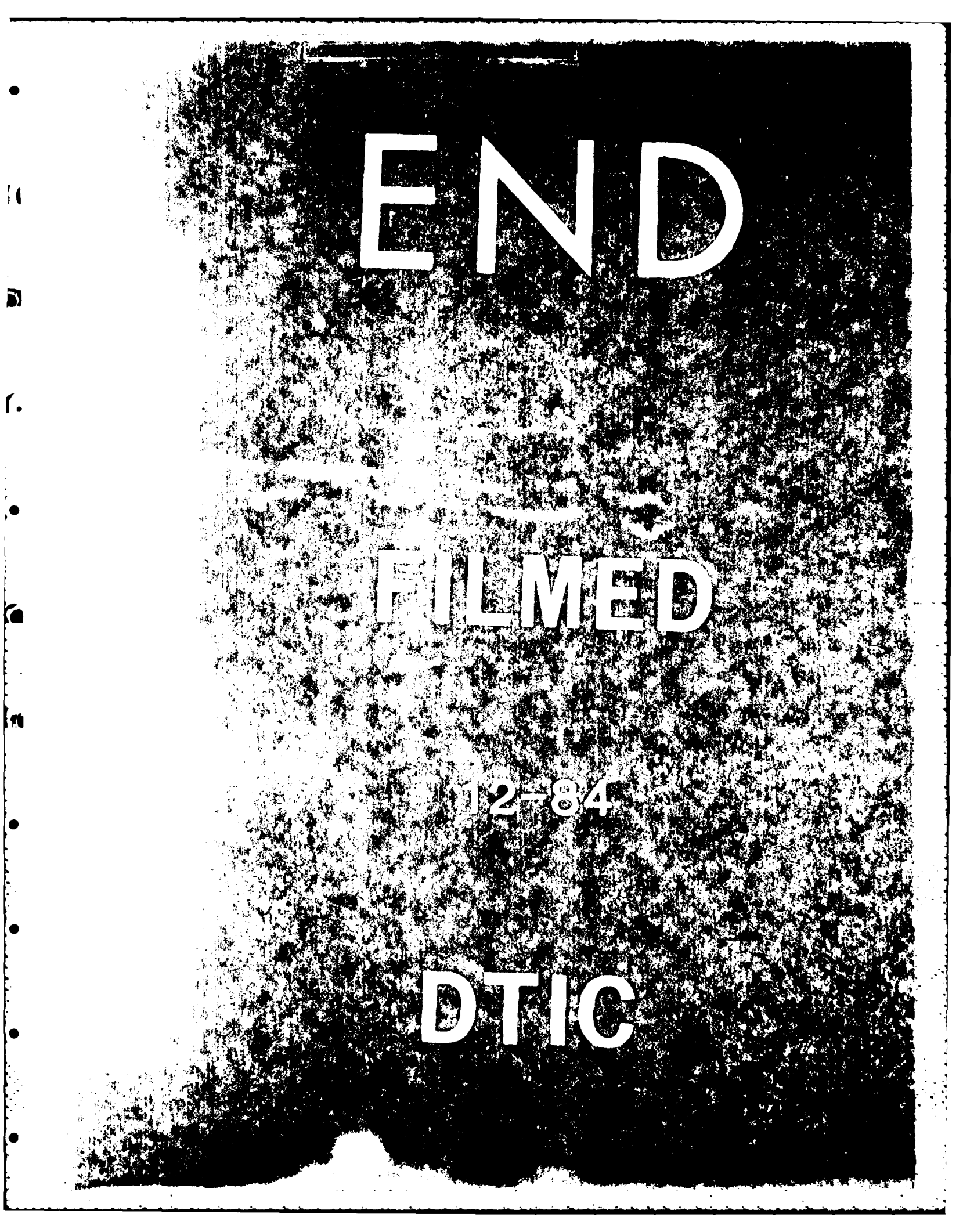
END
FILMED
12-84
DTIC